European Journal of Taxonomy 908: 39–76
https://doi.org/10.5852/ejt.2023.908.2337
ISSN 2118-9773
www.europeanjournaloftaxonomy.eu
2023 · Antić D. *et al.*

Research article

urn:lsid:zoobank.org:pub:1728B5B0-A130-4370-9610-9DA9CEDF4717

Review of the genus *Acanthophorella* Antić & Makarov, 2016 (Diplopoda, Chordeumatida, Anthroleucosomatidae), with descriptions of three new species from the Caucasus

Dragan ANTIĆ [1,*], Mirko ŠEVIĆ [2], Shalva BARJADZE [3] & Slobodan MAKAROV [4]

[1,2,4] University of Belgrade – Faculty of Biology, Institute of Zoology, Studentski Trg 16, 11000 Belgrade, Serbia.
[1,2,4] Serbian Biospeleological Society, Trg Dositeja Obradovića 2, 21000 Novi Sad, Serbia.
[3] Institute of Zoology, Ilia State University, Giorgi Tsereteli 3, 0162, Tbilisi, Georgia.

[*] Corresponding author: dragan.antic@bio.bg.ac.rs
[2] Email: mirko.sevic@bio.bg.ac.rs
[3] Email: shalva.barjadze@iliauni.edu.ge
[4] Email: slobodan@bio.bg.ac.rs

[1] urn:lsid:zoobank.org:author:B5FACDD3-ACCA-4050-8118-80EBD2BB942F
[2] urn:lsid:zoobank.org:author:AE92D931-6893-4884-8173-31C0B5D327FD
[3] urn:lsid:zoobank.org:author:AB36BEF1-C006-41A3-861E-E0B79EE35FBF
[4] urn:lsid:zoobank.org:author:7F5C25A5-615E-427B-B4FC-DB1A0EE1B534

Abstract. The present paper is devoted to the description of three new species of the genus *Acanthophorella* Antić & Makarov, 2016 from Georgia, western Caucasus: *A. devi* Antić sp. nov. and *A. valerii* Antić sp. nov., both presumed troglobionts and each from a single cave, and the epigean *A. aurita* Antić sp. nov. The troglobiotic *Acanthophorella barjadzei* Antić & Makarov, 2016 is reported from two additional caves, with further descriptive notes given. Notes on the ecology and localities, and a distribution map for all six species of the genus are presented. A key is given to all members of the *Flagellophorella* complex. The relationships within the complex and the distribution and troglomorphism in the genus *Acanthophorella* are briefly discussed.

Keywords. Caves, Georgia, *Flagellophorella* complex, millipedes, taxonomy.

Antić D., Šević M., Barjadze S. & Makarov S. 2023. Review of the genus *Acanthophorella* Antić & Makarov, 2016 (Diplopoda, Chordeumatida, Anthroleucosomatidae), with descriptions of three new species from the Caucasus. *European Journal of Taxonomy* 908: 39–76. https://doi.org/10.5852/ejt.2023.908.2337

Introduction

Until recently, the anthroleucosomatid fauna of the Caucasus was poorly studied and included only seven described species. A significant increase in the number of taxa in the group occurred only a few years ago, when Antić & Makarov (2016) described 36 new species and 15 new genera from the Caucasian ecoregion. To date, a total of 20 genera and 45 species of Anthroleucosomatidae Verhoeff, 1899 have been recorded in the Caucasus (Antić & Makarov 2016, 2022; Antić *et al.* 2018). These are all the representatives of the entire order Chordeumatida Pocock, 1894 in the area, apart from one introduced and recently recorded European species from the family Craspedosomatidae (unpubl. data).

Fig. 1. Troglobiotic members of the genus *Acanthophorella* Antić & Makarov, 2016 in situ. **A–B**. *Acanthophorella barjadzei* Antić & Makarov, 2016, ♂ from Nikortsminda Sakinule Cave. **C–D**. *Acanthophorella barjadzei* Antić & Makarov, 2016, ♂ from Muradi Cave. **E–F**. *Acanthophorella devi* Antić sp. nov., types, ♂♂. **G–H**. *Acanthophorella valerii* Antić sp. nov., holotype, ♂ (NHMW MY10366). Photos by Dragan Antić.

In their monograph, Antić & Makarov (2016) classified all anthroleucosomatid genera from the Caucasus into eight endemic complexes. Of these, half are monogeneric, two with two genera each, while the *Caucaseuma* and *Flagellophorella* complexes comprise eight and four genera, respectively. The *Flagellophorella* complex differs from the other Caucasian anthroleucosomatid complexes by the presence of a pair of flagella (*Flagellophorella* Antić & Makarov, 2016), pseudoflagella (*Pseudoflagellophorella* Antić & Makarov, 2016) or processes that can be partially or almost completely hidden inside the angiocoxites of the anterior gonopods (*Acanthophorella* Antić & Makarov, 2016 and *Cryptacanthophorella* Antić & Makarov, 2016) (Antić & Makarov 2016). The genus *Acanthophorella* Antić & Makarov, 2016 is one of the only two genera of Caucasian chordeumatidans that has both troglobiotic and epigean species. The second is *Caucaseuma* Strasser, 1970 (see Antić & Makarov 2022). All three species of *Acanthophorella* described so far are each known from a single locality. Both the epigean *A. chegemi* Antić & Makarov, 2016 and *A. irystoni* Antić & Makarov, 2016 occur in the North Caucasus in Russia, while the troglobiotic *A. barjadzei* Antić & Makarov, 2016 is known from a single cave in the Racha region in western Georgia.

In the present paper we describe three new species of *Acanthophorella* from Georgia, Caucasus, two of which are presumed troglobionts. This brings the number of species in the genus to six, with three epigean and three presumed troglobiotic species (Fig. 1). In addition to the type locality, *A. barjadzei* is recored from two additional caves. We also provide an identification key to all members of the *Flagellophorella* complex and a distribution map for all six known species of the genus *Acanthophorella*.

Material and methods

Preservation, dissecting, imaging, map

Specimens preserved in 70% or 96% ethanol were examined with a Nikon SMZ 745T binocular stereo microscope. All taxonomically important structures were dissected and mounted in glycerine as temporary microscopic preparations and observed with a Carl Zeiss Axioscope 40 microscope. Pictures of the specimens and their relevant habitual structures were taken using a Nikon DS-Fi2 camera with a Nikon DS-L3 camera controller attached to a Nikon SMZ 1270 binocular stereo microscope. Pictures of legs and gonopods were made with a Canon PowerShot A80 digital camera connected to a Carl Zeiss Axioscope 40 microscope. All pictures were stacked with a Zerene Stacker. Line drawings of the gonopods and vulvae were obtained using tracing paper placed on a computer monitor displaying pictures of those structures made with a Canon PowerShot A80 digital camera connected to a Carl Zeiss Axioscope 40 microscope. Samples for scanning electron microscopy (SEM) were mounted on aluminium stubs equipped with sticky aluminium tape, air-dried, coated with gold (BAL-TEC SCD005 Sputter Coater) and studied with a JEOL JSM-6460LV scanning electron microscope (University Center for Electron Microscopy, Department of Biology and Ecology, University of Novi Sad, Serbia). After SEM examination, all parts were put back into ethanol. The photos of the living animals in situ were taken with an Olympus Stylus Tough TG-6 digital camera. The images were processed and assembled in Adobe Photoshop CS6.

The structures of the gonopods and vulvae in the SEM photographs are slightly deformed due to shrinkage; the best indication of what the shapes really look like are the drawings.

The distribution map was created using Google Earth Pro (ver. 7.3.4.8248) and Adobe Photoshop CS6. The final images were processed with Adobe Photoshop CS6.

Abbreviations of gonopodal and vulval structures

Anterior gonopods

a = angiocoxite
ap = anterior process

cv = coxal/syncoxal vesicle
ll = lateral lamella
mp = medial part
pl = posterior lobe
s = sternum
sa = synangiocoxal base
sl = sternal lamella
tf = angiocoxal tuft

Posterior gonopods

a = angiocoxite
ap = anterior process
c = colpocoxite
cv = coxal vesicle
s = sternum
t = telopodite (remnants)

Vulvae

b = bursa
o = operculum

Abbreviations of indices of body ring 15

CIX = macrochaetal index = distance between exterior and median macrochaetae/distance between interior and median macrochaetae
MA = macrochaetal angle = angle between the arm created by the median and exterior macrochaetae and the arm formed by the median and interior macrochaetae
MIX = median index = distance between interior macrochaetae and axial suture/distance between interior and median macrochaetae
PIX = paratergal index = (width of metazonite – width of prozonite)/(2× length of paratergum)

Museum and collection acronyms

IZB = Institute of Zoology, University of Belgrade – Faculty of Biology, Belgrade, Serbia
IZISU = Institute of Zoology, Ilia State University, Tbilisi, Georgia
NHMW = Naturhistorisches Museum Wien, Vienna, Austria
SMNG = Senckenberg Museum of Natural History, Görlitz, Germany
SMNS = Stuttgart State Museum of Natural History, Stuttgart, Germany

Results

Class Diplopoda de Blainville in Gervais, 1844
Order Chordeumatida Pocock, 1894
Suborder Craspedosomatidea Cook, 1895
Superfamily Anthroleucosomatoidea Verhoeff, 1899
Family Anthroleucosomatidae Verhoeff, 1899

Genus ***Acanthophorella*** Antić & Makarov, 2016

Acanthophorella Antić & Makarov, 2016: 142.

Type species

Acanthophorella barjadzei Antić & Makarov, 2016, by original designation.

Diagnosis

The genus *Acanthophorella* belongs to the *Flagellophorella* complex which differs from other Caucasian Anthroleucosomatidae by the presence of a pair of anterior flagella, pseudoflagella or processes that can be partially covered by or almost completely hidden inside the angiocoxites of the anterior gonopods. This genus differs from the other three genera of the complex by the presence of a pair of mainly spinelike acuminate or tapering processes arising from the synangiocoxal base on the anterior side of the angiocoxites of the anterior gonopods [vs presence of a pair of flagella in *Flagellophorella*, a pair of pseudoflagella (very long, equally thick over the entire height) in *Pseudoflagellophorella* (Fig. 21G–I) or a pair of hidden processes with only their distal parts visible in *Cryptacanthophorella*].

In comparison with the most similar genus, *Pseudoflagellophorella*, it seems that the main and apparently only difference lies in the structure of the processes of the angiocoxites of the anterior gonopods. In the genus *Acanthophorella*, these processes are mostly stubby (except perhaps in *A. barjadzei* with somewhat more slender ones) arising directly distad from the lateral parts of the synangiocoxal base and tapering in all species, mostly acuminate. In the genus *Pseudoflagelophorella*, these processes are very slender, without synangiocoxal base, not tapering but of equal thickness over the entire height and starting a little closer to the medial part of the angiocoxites, where they first form a semicircular curvature and then rise distad.

Remarks

With the three additional species described below, it would seem that the differences between the genera *Acanthophorella* and *Pseudoflagellophorella* are becaming minor if any. For the time being, however, we shall keep both genera as valid, although it is possible that they will be synonymised in the future when more material becomes available. This also applies to the genus *Cryptacanthophorella*. With this in mind, when diagnosing new species here, we shall compare them with species of both *Acanthophorella* and *Pseudoflagellophorella*, although the new species are quite remarkable.

Other species included

Acanthophorella aurita Antić sp. nov.
Acanthophorella devi Antić sp. nov.
Acanthophorella valerii Antić sp. nov.
Acanthophorella chegemi Antić & Makarov, 2016
Acanthophorella irystoni Antić & Makarov, 2016

Descriptions of new species and their ecology

Acanthophorella aurita Antić sp. nov.
urn:lsid:zoobank.org:act:ADCB7F33-A824-42E3-B7F5-D2EA41BC93DA
Figs 2–5, 21A, 22

Diagnosis

Distinguished from congeners and members of the genus *Pseudoflagellophorella* by the presence of very characteristic, wide, more or less ear-shaped angiocoxites of the posterior gonopods in anterior or posterior views (vs angiocoxites are more or less slender or small in all other members of the genera *Acanthophorella* and *Pseudoflagellophorella*).

Etymology

From Latin '*auris*' ('ear') + '-*ītus*'; '*aurita*' (= 'earlike'; having ears or having the shape of a ear) because of the characteristic shape of the angiocoxites of the posterior gonopods. Feminine adjective.

Material examined

Holotype

GEORGIA • ♂; Samegrelo-Zemo Svaneti, Khobi Municipality, Urta Mts, small cavity near the ruins of Jegeta church (Jegeta 2 Cave); 21 Oct. 2021; J. Grego and M. Szekeres leg.; NHMW MY10363.

Description

Size and number of body rings. Body with 31 rings (including telson), length: 10.5 mm, vertical diameter of the largest ring 1.0 mm.

Coloration (Fig. 2). With brownish, greyish and yellowish patterns. Ommatidia black.

Head (Fig. 2B–C). Setose, frontal side with a slight medial concavity and with a rectangular lobe (Fig. 2C, white arrows), below each antennal socket. Labrum with three medial teeth and 5+4 labral and 2+2 supralabral setae. Promentum triangular, without setae. Lamellae linguales with 4+4 setae. Stipites with ca 20 setae each. Antennae 1.8 mm long. Length of antennomeres (in mm): I (0.08), II (0.2), III (0.53), IV (0.22), V (0.47), VI (0.13), VII (0.14) and VIII (0.03). Length/breadth ratios of antennomeres I–VII: I (1), II (2), III (5), IV (2.2), V (3.6), VI (1) and VII (1.5). Antennomeres II, IV, V, VI and VII with one, three, one, four and one long sensillum trichoideum, respectively. Antennomere 7 with one rather bacilliform sensillum (sensillum basiconicum?) curved distad, located below sensillum trichodeum. Lateral to antennal sockets a group of papilliform outgrowths present. Number of ommatidia: 12+13 in 3 or 4 rows, arranged in elongated triangles (Fig. 2B–C).

Collum. Narrower than head, with six macrochaetae as all body rings. Anterior edge semi-circular, posterior margin gently concave.

Body rings (Fig. 2A, D–E). With well-developed lateral keels. Macrochaetae long and rather rodlike, with longitudinal ribs, ending with spikes. CIX (ring 15) = 0.5; MIX (ring 15) ~ 1.5; PIX (ring 15) = 0.7; MA (ring15) ~ 100°.

Telson. Epiproct with a pair of spinnerets and 3+3 setae (1+1 paramedian, 2+2 marginal). Hypoproct with 1+1 distal setae. Paraprocts with 3+3 marginal setae in distal part.

Leg-pairs 1 and 2. With tarsal combs; femora, postfemora and tibiae with long and robust setae.

Male sexual characters (Figs 2A, 3). Gonopores mesally on coxae 2 (Fig. 3A). Leg-pairs 3–7 enlarged, especially leg-pairs 3, 4 and 7 (Fig. 2A). Leg-pairs 3 and 4 very thick, each with a proximal lateral protrusion on prefemora; prefemora and femora strong, rectangular; tarsi shorter and thicker compared to other legs (Fig. 3B). Leg-pair 3 with a distoventral femoral pad (Fig. 3B–C); observed on neither other podomeres nor legs. Leg-pair 4 with a mesal concavity on prefemora and femora. Leg-pair 5 with a proximal, anterior, triangular coxal protrusion. Leg-pair 6 without peculiarities. Leg-pair 7 robust; coxae with well-developed, subrectangular, flattened posterior processes, covered with long setae anteriorly, each with a lateral tooth curved anteriad (Fig. 3D). Leg-pair 10 with coxal glands and with a bilobed protrusion, triangular anteriorly and rounded posteriorly, both lobes covered with tubercules (Fig. 3E, only anterior, triangular part of lobe visible). Leg-pair 11 with coxal glands, no other peculiarities.

Anterior gonopods (Figs 4A, C, 5A–C, 21A). Gonopodal sternum (s) wide, medially with a well-developed, subtriangular, fimbriate lamella (sl) on anterior side. Angiocoxites (a) consisting of a medial part (mp), lateral lamellae (ll) and a synangiocoxal base with anterior processes (ap). Medial parts well-developed, divided, but appressed to each other, shield like, tapering distolaterally into hook-shaped processes in anterior and posterior views, curved sharply proximad and posteriad; distally these

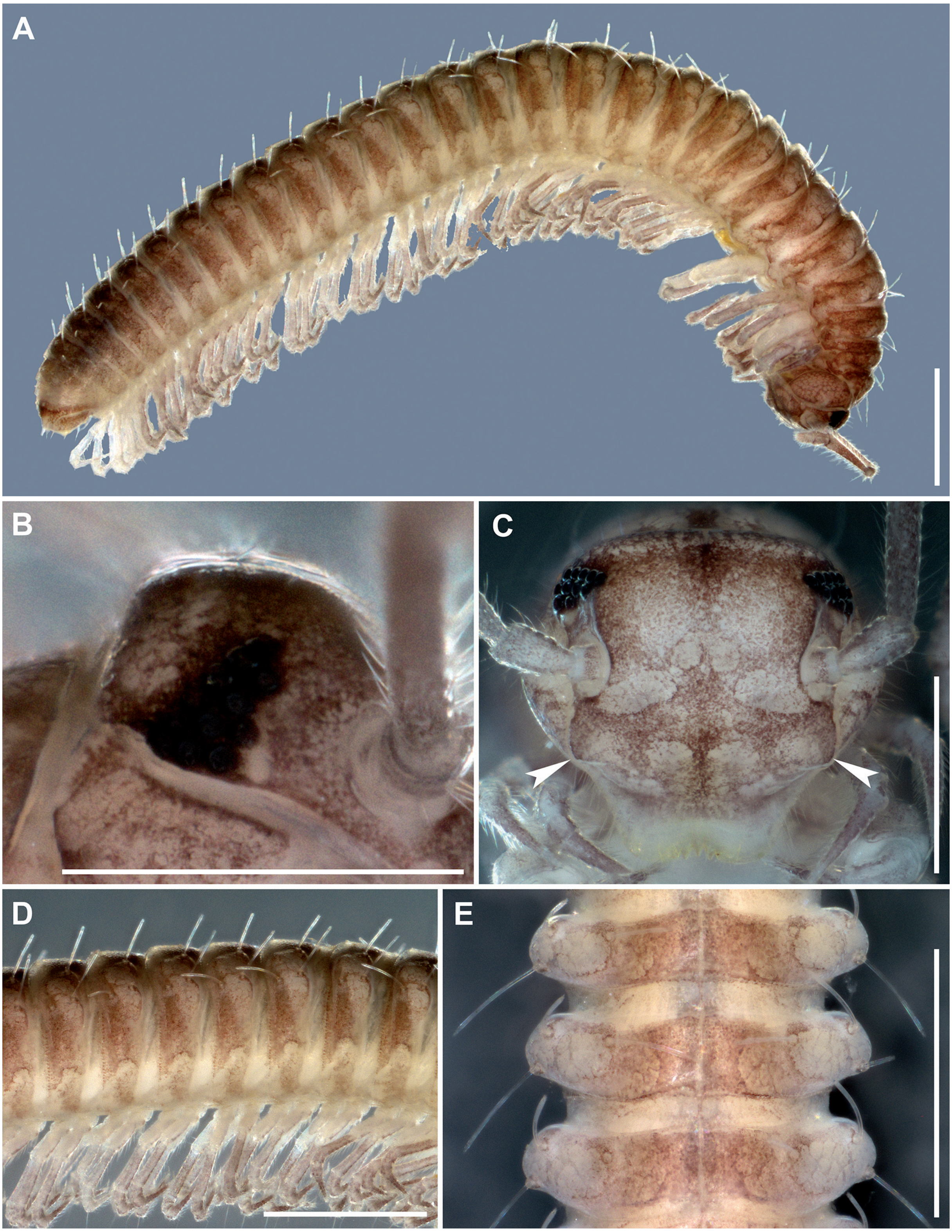

Fig. 2. *Acanthophorella aurita* Antić sp. nov., holotype, ♂ (NHMW MY10363). **A**. Habitus, lateral view. **B**. Right field with ommatidia, lateral view. **C**. Head, anterior view, white arrows indicate rectangular lobes. **D**. Midbody rings, lateral view. **E**. Midbody rings, dorsal view. Scale bars: A, D–E = 1 mm; B–C = 0.5 mm.

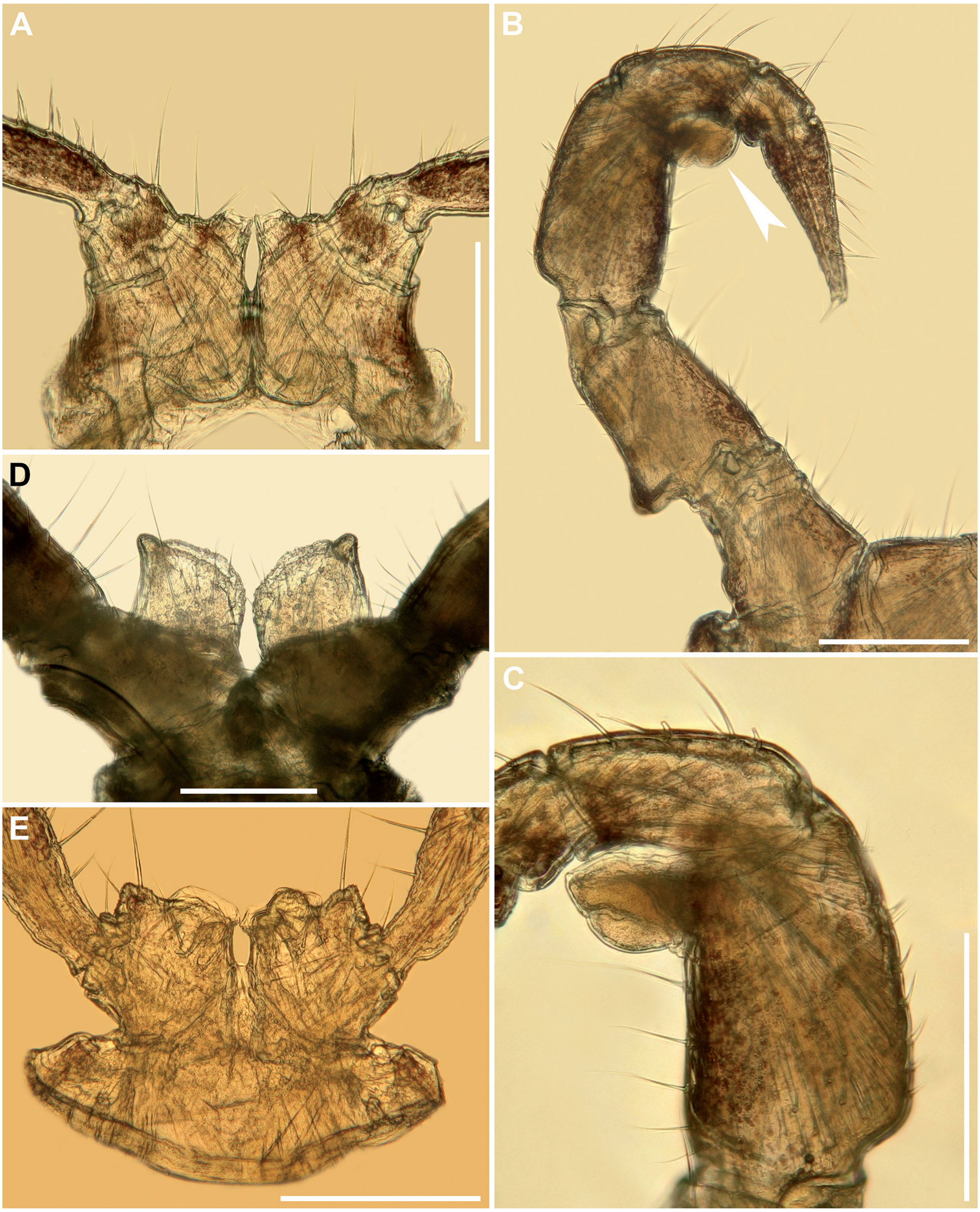

Fig. 3. *Acanthophorella aurita* Antić sp. nov., holotype, ♂ (NHMW MY10363). **A**. Leg-pair 2, posterior view. **B**. Left leg 3, anterior view, white arrow indicates the distoventral femoral pad. **C**. Right leg 3 with a distoventral femoral pad, anterior view. **D**. Leg-pair 7, anterior view. **E**. Leg-pair 10, anterior view. Scale bars = 0.2 mm.

processes wide, rather spoon-shaped; distomesal margins folded posteriad; additional three processes can be seen posteriorly (best seen in lateral view); angiocoxites posteroproximally with a pair of tufts (tf) with hairlike outgrowths. Lateral lamellae high, curving posterolaterad into two strongly developed layers of fringed extension. Anterior processes (ap) tapering distad, blunt, short, high as half as height of medial angiocoxal part. Coxal vesicle (?) (cv) poorly developed.

Posterior gonopods (Figs 4B, D, 5D–E). Gonopodal sternum (s) wide, well-developed. Angiocoxites (a) strongly developed, more or less ear-shaped in anterior and posterior views, with lateral and distal margins curved anteriad; proximally with a short anterior process (ap). Coxal vesicles (cv) poorly developed, visible on mesal sides of angiocoxites at their mid-height. Telopodites (t) reduced to pigment remnants (a claw is visible on the right side).

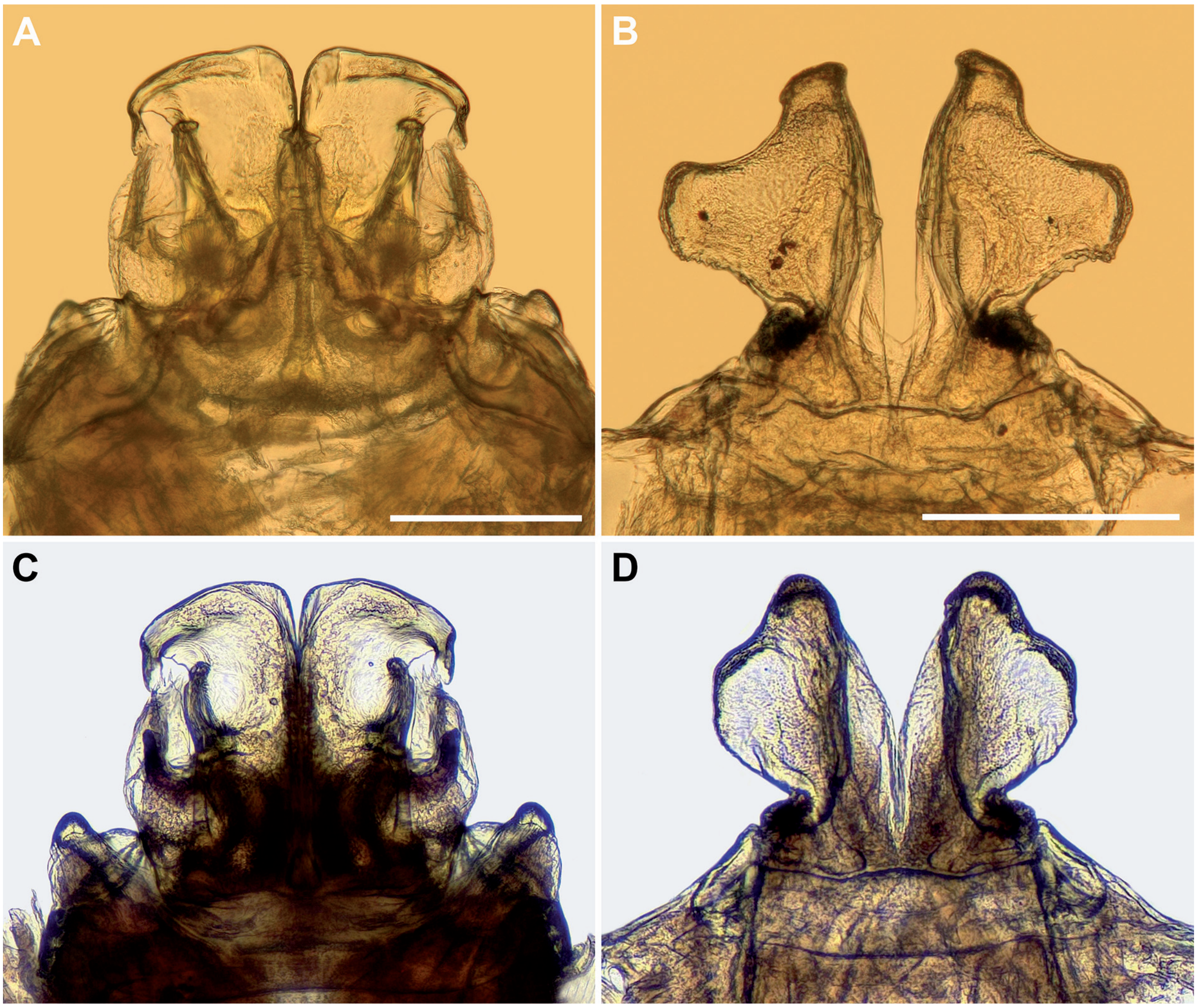

Fig. 4. A–B. *Acanthophorella aurita* Antić sp. nov., holotype, ♂ (NHMW MY10363). **C–D**. *Acanthophorella* cf. *A. aurita* from Kveda Tlughi. **A, C**. Anterior gonopods, anterior and posterior views, respectively. **B, D**. Posterior gonopods, anterior views. Scale bars = 0.2 mm; C–D not to scale.

Remarks

An apparently conspecific specimen was found in the forest, near the Cholaga spring, village Kveda Tlughi, in the Racha region. This locality is about 100 air-km from the type and only locality of *A. aurita* sp. nov. Unfortunately, the sample from Kveda Tlughi is considered lost in the IZISU collection. From the available pictures of the gonopods alone (Fig. 4C–D) it is evident that both males are very similar, although the shape of the angiocoxites of the posterior gonopods is slightly different. Additional males from both localities, as well as in between, could clarify whether it is only a variation in the shape of the angiocoxites of the posterior gonopods, which seems most likely. The locality Kveda Tlughi is marked with a question mark on the map for *A. aurita* for the time being.

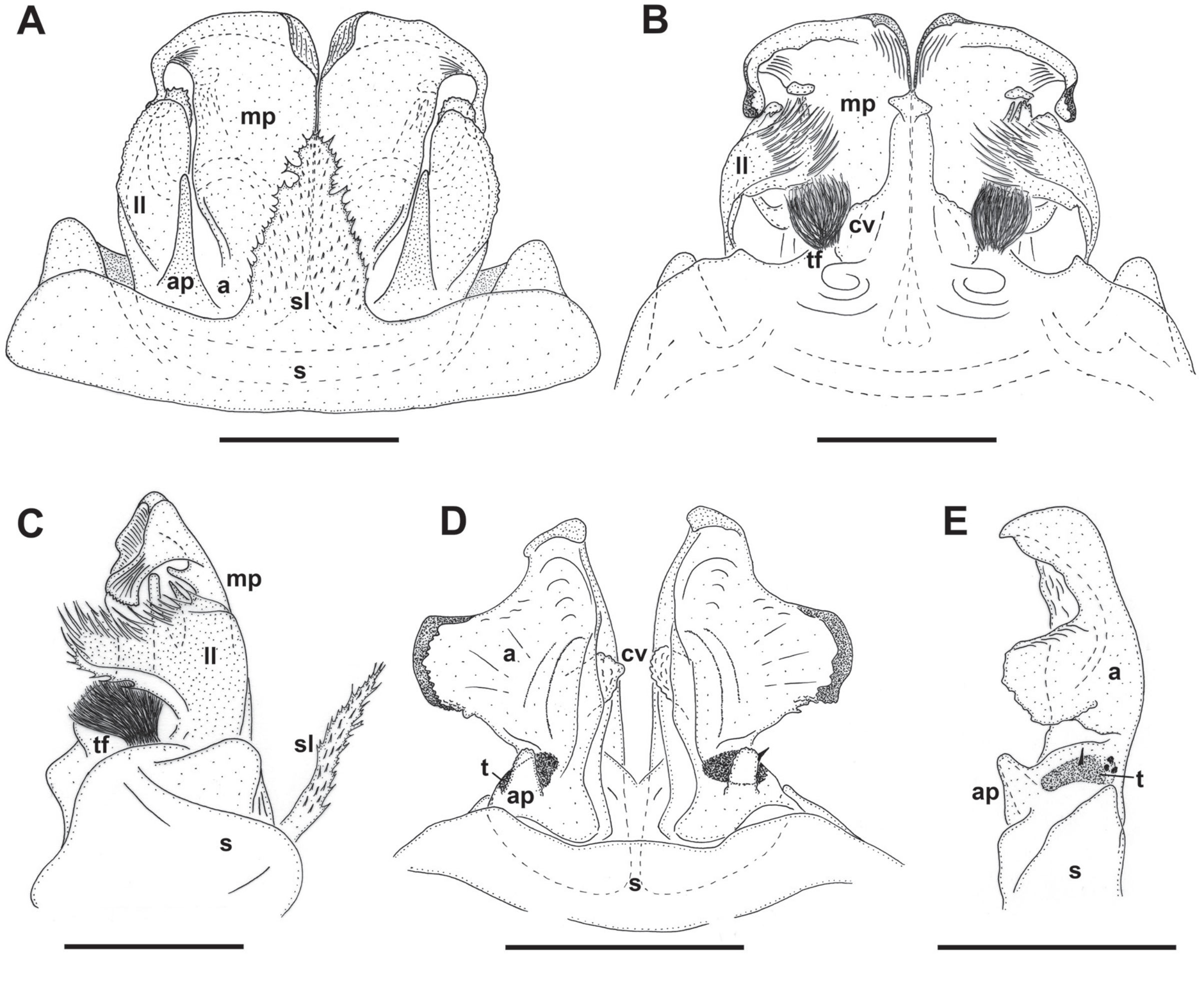

Fig. 5. *Acanthophorella aurita* Antić sp. nov., holotype, ♂ (NHMW MY10363), gonopods. **A**. Anterior gonopods, anterior view. **B**. Anterior gonopods, posterior view. **C**. Anterior gonopods, lateral view. **D**. Posterior gonopods, anterior view. **E**. Right posterior gonopod, lateral view. Abbreviations: a = angiocoxite; ap = anterior process; cv = coxal vesicle; ll = lateral lamella; mp = medial part; s = sternum; sl = sternal lamella; t = telopodital pigment remnants; tf = angiocoxal tuft. Drawings by DA. Scale bars = 0.2 mm.

Near the type locality, in Urta (= Jegeta 1) Cave, we recorded a larger number of juveniles (five collected, IZISU) during the 2022 expedition, but in the absence of an adult male we shall not assign these specimens to *A. aurita* sp. nov., although it is very likely that they are the same species.

Localities and ecology

The holotype male was collected in a small, slightly descending cavity with a small entrance, and with a hall about 3–3.5 mm long and 1.5–2 m wide. This cavity is characterised by an additional small opening on the ceiling, causing the floor to be covered with moist, black, humic soil with leaf litter and a thin layer of dead leaves. The specimen was found in this substrate (Jozef Grego pers. com.). Another millipede found in the cavity was *Pachyiulus krivolutskyi* Golovatch, 1977, a common epigean species in the western Caucasus. The cavity is tentatively named Jegeta 2 Cave or Cave 2 near the ruins of Jegeta church. The sample from Kveda Tlughi, which is most likely *A. aurita* sp. nov., as well, came from sieving leaf litter. In the Urta (= Jegeta 1) cave, juveniles of possibly this species were observed only in and on dead wood in the cave, but very close to the entrance.

This species is an epigean member of the genus *Acanthophorella* and as juveniles possibly belonging to this species were found in the cave, it may be considered troglophilic.

Distribution

A Georgian endemic known from the Urta Mountains (Khobi Municipality) and possibly from Kveda Tlughi (Ambrolauri Municipality) (Fig. 22, green circles).

Acanthophorella devi Antić sp. nov.
urn:lsid:zoobank.org:act:DDAE0A65-7AB2-42AF-914C-1CE779454840
Figs 1E–F, 6–10, 21D, 22

Diagnosis

Distinguished from congeners and members of the genus *Pseudoflagellophorella* by the presence of a poorly developed or the complete absence of a protrusions on coxae 10 in males (Fig. 8E, vs presence of well-developed subtriangular or rounded protrusion or even a long process in congeners or members of *Pseudoflagellophorella*) and, aside from *A. barjadzei* and *A. valerii* sp. nov., by a whitish and unpigmented body (vs pigmented body in others). From *A. valerii*, it differs by the presence of pale brownish ommatidia (vs black in *A. valerii*), the absence of a mesal tooth on the coxal processes of leg-pair 7 (vs presence in *A. valerii*) and in the general shape of the anterior and posterior gonopods. From the most similar *A. barjadzei* (in terms of anterior and posterior gonopods), *A. devi* sp. nov. differs in the absence of a mesal tooth on the coxal processes of leg-pair 7 (vs presence in *A. barjadzei*), as well as in the general appearance: *A. devi* is smaller, 11–13 mm long (vs 16–26 mm in *A. barjadzei*), by the shape of paranota, and by the shorter and rodlike, rather bacilliform macrochaetae (vs longer trichoid macrochaetae in *A. barjadzei*).

Etymology

In Georgian mythology, Devi ('დევი') is a many-headed malevolent giant who lives in the underworld. The type locality Devis Khvreli ('დევის ხვრელი') means 'Devi's hole'. Noun in apposition.

Material examined

Holotype

GEORGIA • ♂; Imereti Region, Chiatura Municipality, Zemo Imereti plateau karst massif, Rgani village, Devis Khvreli Cave; 691 m a.s.l.; 26 Jul. 2022; D. Antić, E. Kiria and L. Shavadze leg.; NHMW MY10364.

Paratypes

GEORGIA • 1 ♂, 1 ♀ (used for SEM); same collection data as for holotype; IZB • 1 ♂, 1 ♀; same collection data as for holotype; IZISU • 1 ♀; same collection data as for holotype; NHMW MY10365.

Additional material

GEORGIA • 1 ♂, 5 juvs; same cave as for holotype; 23 Nov. 2018; G. Nebieridze leg.; IZISU.

Description

Size and number of body rings. Body with 31 rings (including telson). Holotype male 11 mm long, vertical diameter of the largest ring 0.80 mm. Paratype males 12–13 mm long, vertical diameter of the largest ring 0.85–0.90 mm, respectively. Paratype females 12–13 mm long, vertical diameter of the largest ring 0.90–0.95 mm, respectively.

Coloration (Figs 1E–F, 6). Living animals white with pale brownish ommatidia.

Head (Figs 6A–B, 7A–D). Setose, roundly convex in females, in males with labral and frontal surfaces flat with a convexity between and with a pair of lateral lobes, each below antennal sockets. Labrum with three medial teeth and 5+5 labral and 2+2 supralabral setae. Promentum triangular, without setae. Lamellae linguales with 7+6 setae. Stipites with ca 25 setae each. Antennae 2 mm long in holotype male. Length of antennomeres (in mm): I (0.1), II (0.2), III (0.55), IV (0.27), V (0.5), VI (0.17), VII (0.17) and VIII (0.04). Length/breadth ratios of antennomeres I–VII: I (1), II (1.5), III (5.5), IV (2.7), V (3.5), VI (1.1) and VII (1.5). Antennomeres II, IV, V, VI and VII with one, three, one, four and one long sensillum trichoideum, respectively. Antennomere 7 with one rather bacilliform sensillum (sensillum basiconicum?) curved distad, located below sensillum trichodeum. Lateral to antennal sockets, a group of papilliform outgrowths present. Number of ommatidia: 5–7 in 2–3 irregular rows (Figs 6A, 7C–D).

Collum. Narrower than head, with six macrochaetae as all body rings. Anterior edge semi-circular, posterior margin gently concave.

Body rings (Figs 6A, C–E, 7E–H). With well-developed lateral keels, rounded in dorsal view. Macrochaetae rather short and rodlike, with longitudinal ribs, ending with spikes (Fig. 7H). CIX (ring 15) = 0.6; MIX (ring 15) ~ 1.5; PIX (ring 15) = 0.6; MA (ring 15) ~ 100°.

Telson. Epiproct with a pair of spinnerets and 3+3 setae (1+1 paramedian, 2+2 marginal). Hypoproct with 1+1 distal setae. Paraprocts with 3+3 marginal setae in distal part.

Leg-pairs 1 and 2. In both sexes with tarsal combs; femora, postfemora and tibiae with long and robust setae.

Male sexual characters (Figs 1E–F, 8B–E). Gonopores mesally on coxae 2 (Fig. 8B). Leg-pairs 3–7 enlarged, especially leg-pairs 3, 4 and 7 (Fig. 1E–F). Leg-pairs 3 and 4 very thick, each with a proximal lateral protrusion on prefemora; prefemora and femora strong, rectangular; tarsi shorter and thicker compared to other legs; femora, postfemora and tibiae each with a distoventral pad (Fig. 8C, arrows indicate distoventral pads). Leg-pair 5 with a proximal, somewhat elongated, anterior, triangular, coxal protrusion (Fig. 1E). Leg-pair 6 without peculiarities. Leg-pair 7 robust; coxae with wide, well-developed, flattened posterior processes, covered with long setae anteriorly and with a lateral lobe giving the impression of a subtriangular appereance (Fig. 8D). Leg-pair 10 with coxal glands and a poorly developed or completely absent protrusion (Fig. 8E). Leg-pair 11 with coxal glands, no other peculiarities.

Anterior gonopods (Figs 8F, 9A–F, 10A–C, 21D). Gonopodal sternum (s) wide, medially with a poorly-developed, low, fimbriate lamella (sl) on anterior side. Angiocoxites (a) consisting of a medial part (mp), lateral lamellae (ll) and a synangiocoxal base with anterior processes (ap). Medial parts well-developed,

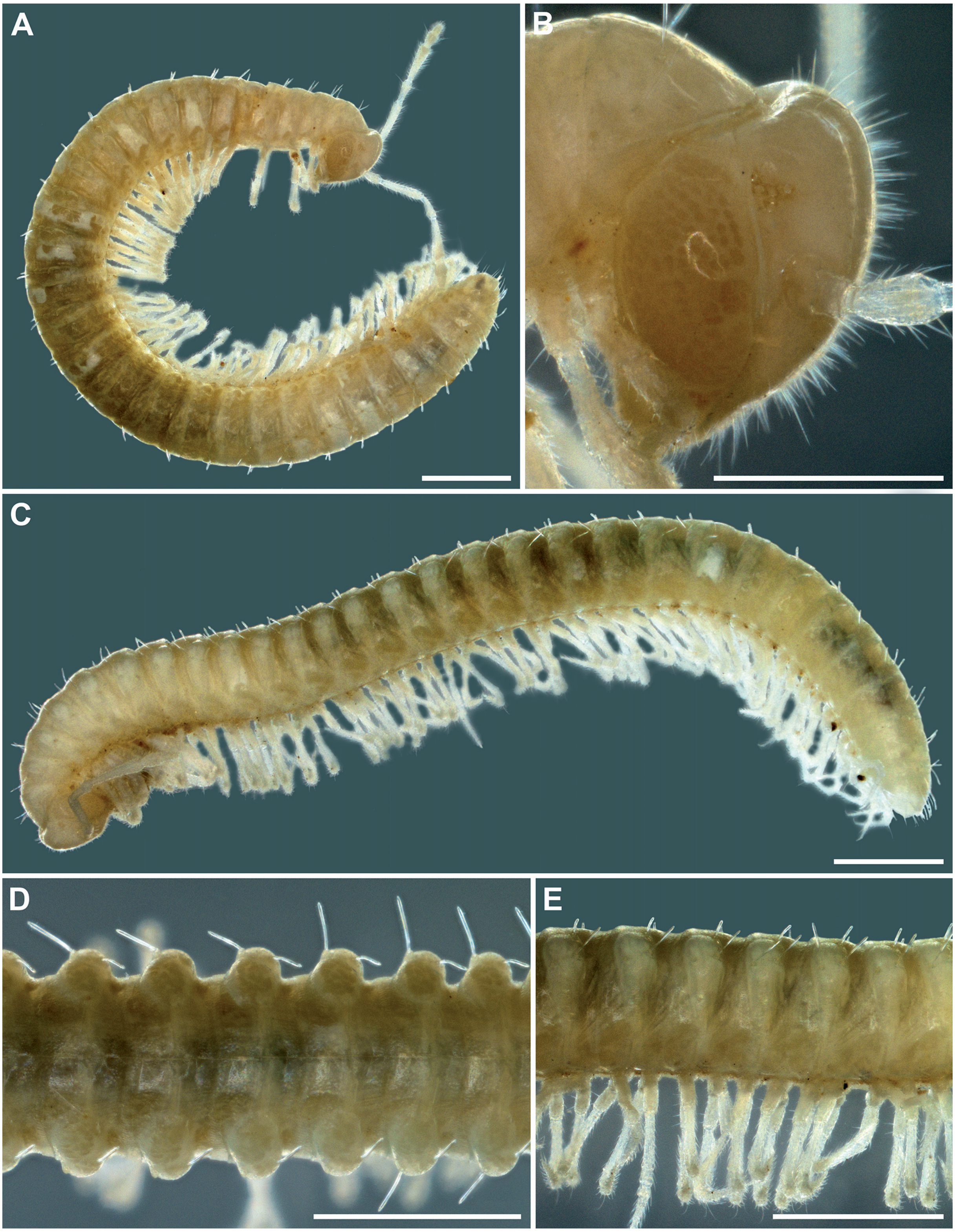

Fig. 6. *Acanthophorella devi* Antić sp. nov. **A–B**. Paratype, ♀ (IZB). **C–E**. Holotype, ♂ (NHMW MY10364). **A**. Habitus, lateral view. **B**. Head and collum, lateral view. **C**. Habitus, lateral view. **D**. Midbody rings, dorsal view. **E**. Midbody rings, lateral view. Scale bars: A, C–E = 1 mm; B = 0.5 mm.

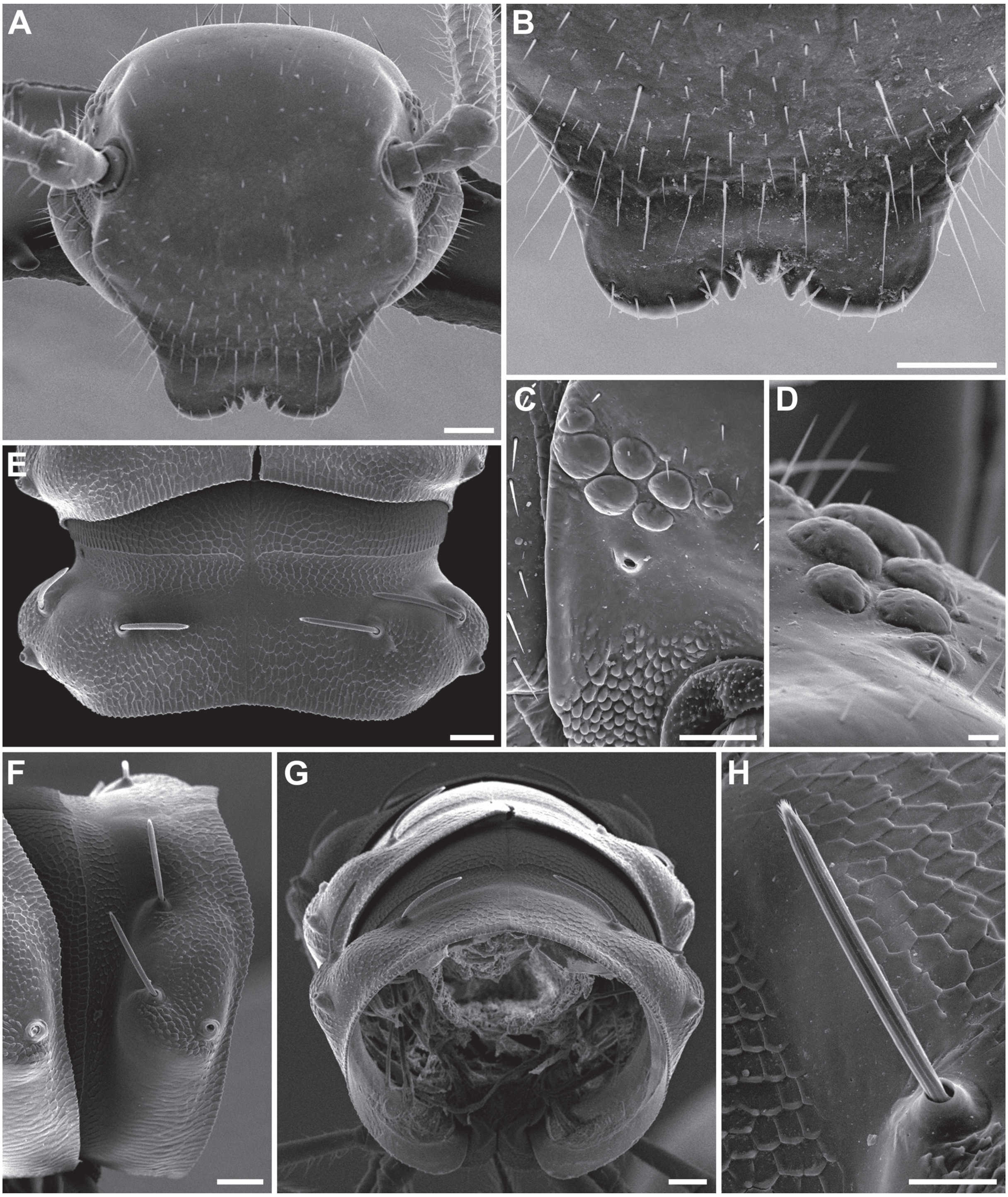

Fig. 7. *Acanthophorella devi* Antić sp. nov., paratype, ♂ (IZB). **A**. Head, anterior view. **B**. Labrum, anterior view. **C**. Right side of head showing field with ommatidia, organ of Tömösvary and group of papilliform outgrowths, lateral view. **D**. Right field with ommatidia, anterior view. **E**. Ring 16, dorsal view. **F**. Ring 16, dorsolateral view. **G**. Rings 14–16, posterior view. **H**. Left interior macrochaeta of ring 15, lateral view. Scale bars: A–B, E–G = 0.1 mm; C, H = 0.05 mm; D = 0.01 mm.

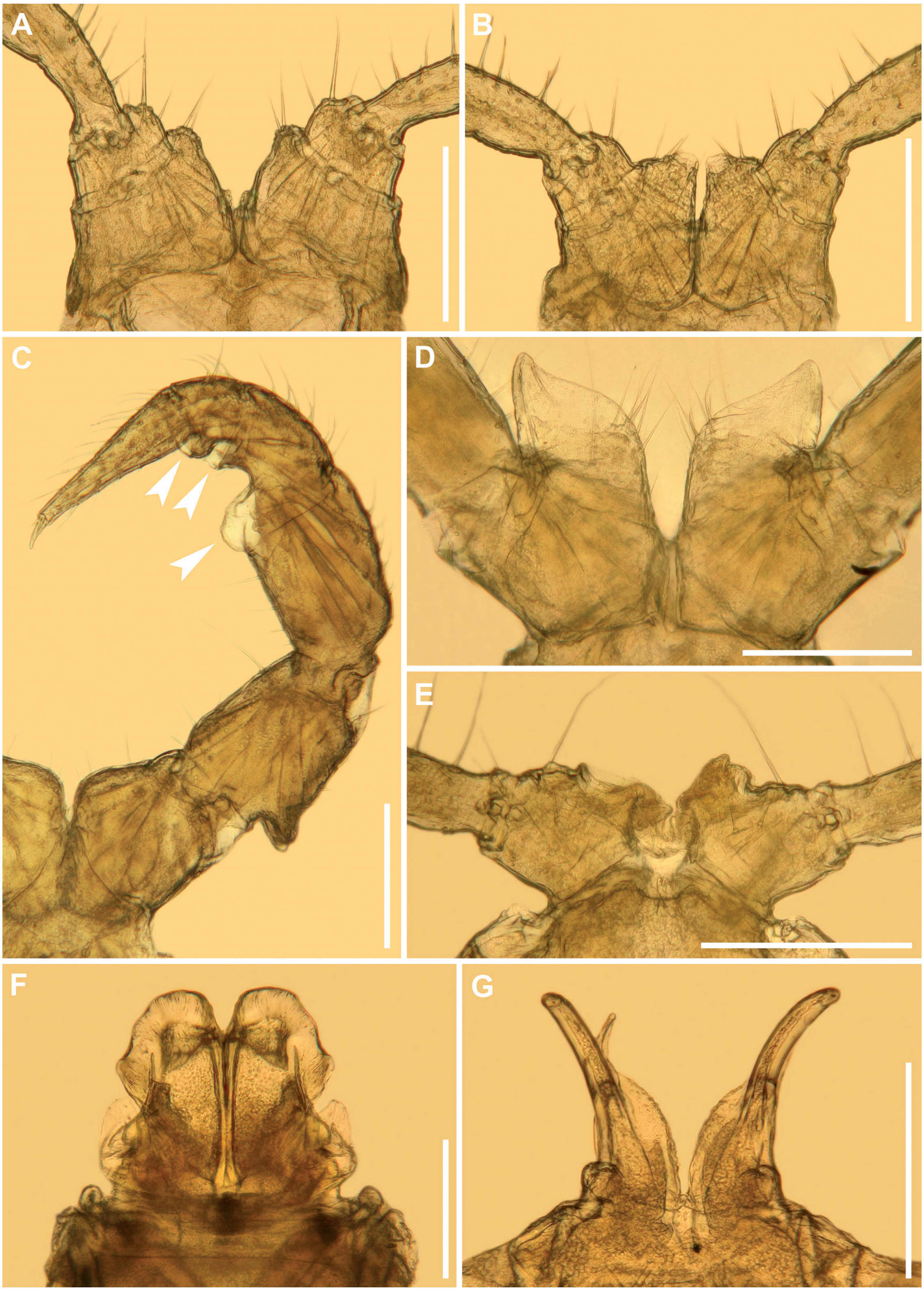

Fig. 8. *Acanthophorella devi* Antić sp. nov. **A**. Paratype, ♀ (IZB), **B–G**. Paratype, ♂ (IZB). **A**. Leg-pair 2, anterior view. **B**. Leg-pair 2, anterior view. **C**. Right leg 4, anterior view, white arrows indicate distoventral pads. **D**. Leg-pair 7, posterior view. **E**. Leg-pair 10, anterior view. **F**. Anterior gonopods, anterior view. **G**. Posterior gonopods, posterior view. Scale bars = 0.2 mm.

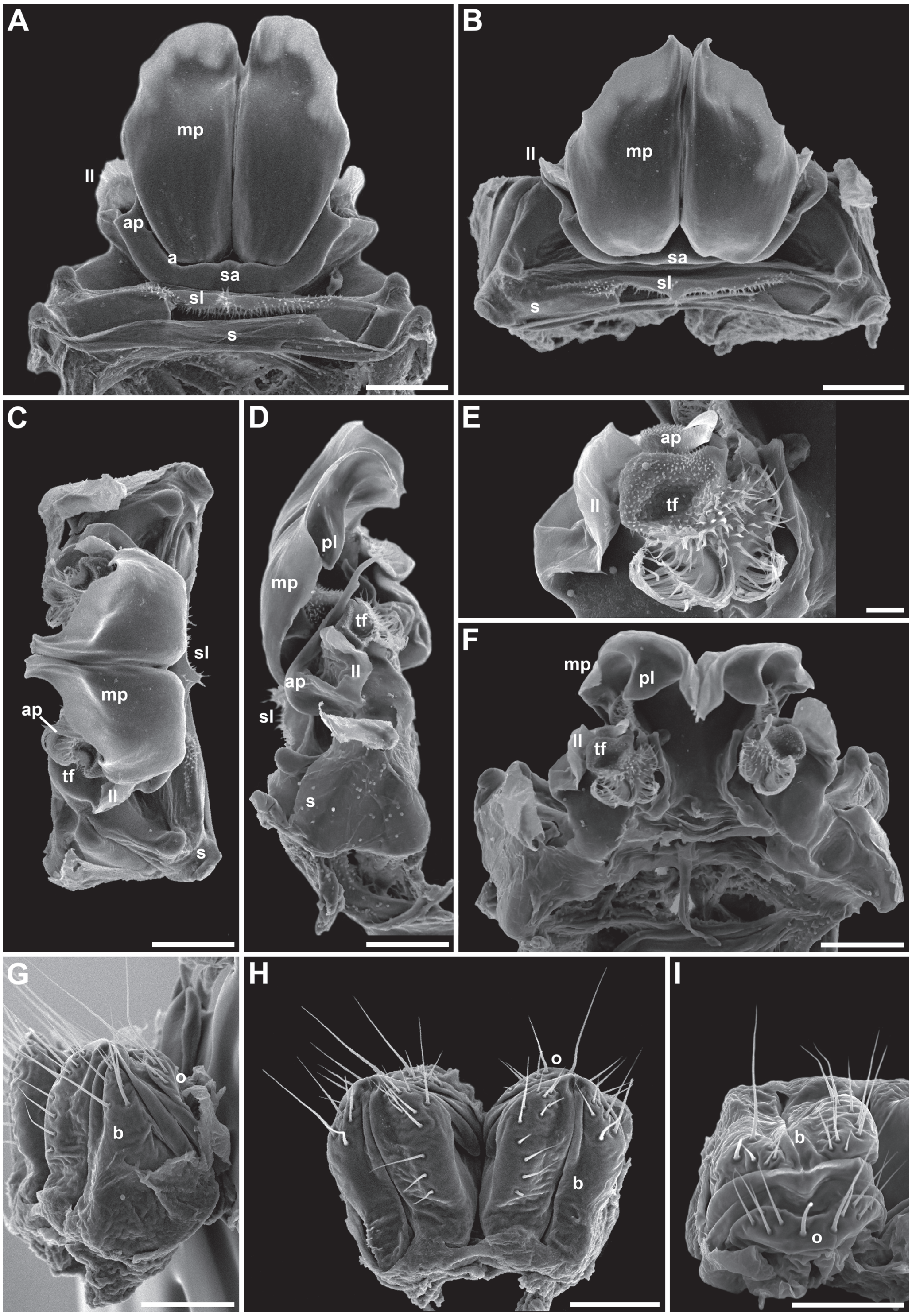

Fig. 9. *Acanthophorella devi* Antić sp. nov. **A**–**F**. Paratype, ♂ (IZB). **G**–**I**. Paratype, ♀ (IZB). **A**. Anterior gonopods, anterior view. **B**. Anterior gonopods, anterodistal view. **C**. Anterior gonopods, distal view. **D**. Anterior gonopods, lateral view. **E**. Anterior gonopods, lateral lamella and tuft, posterodistal view. **F**. Anterior gonopods, posterodistal view. **G**. Left vulva, lateral view. **H**. Vulvae, distal view. **I**. Left vulva, anterior view. Abbreviations: a = angiocoxite; ap = anterior process; b = bursa; ll = lateral lamella; mp = medial part; o = operculum; pl = posterior lobe; s = sternum; sa = synangiocoxal base; sl = sternal lamella; tf = angiocoxal tuft. Scale bars: A–D, F–I = 0.1 mm; E = 0.02 mm.

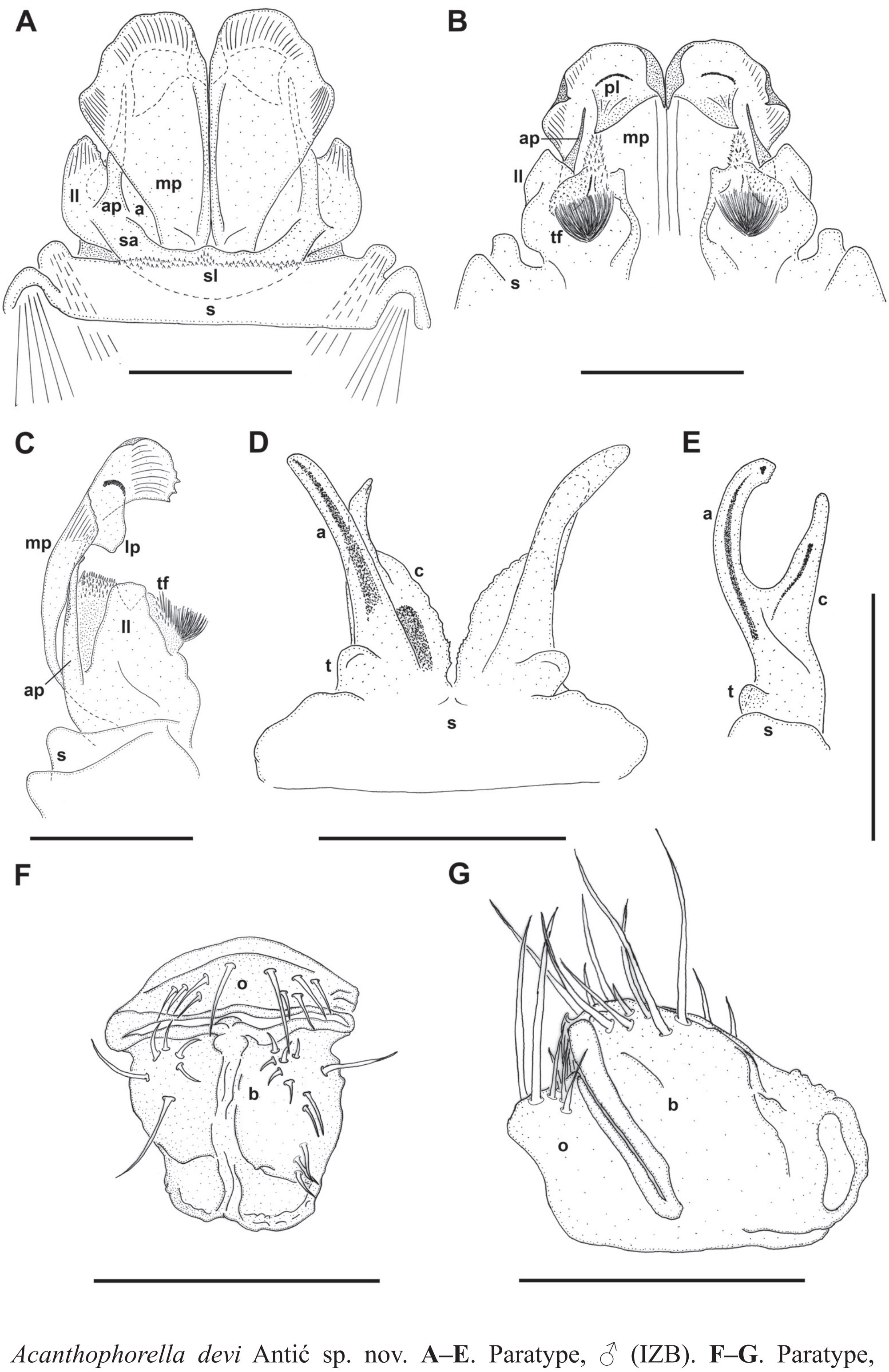

Fig. 10. *Acanthophorella devi* Antić sp. nov. **A–E**. Paratype, ♂ (IZB). **F–G**. Paratype, ♀ (IZB). **A**. Anterior gonopods, anterior view. **B**. Anterior gonopods, posterior view. **C**. Anterior gonopods, lateral view. **D**. Posterior gonopods, posterior view. **E**. Left posterior gonopod, lateral view. **F**. Right vulva, distal view. **G**. Right vulva, lateral view. Abbreviations: a = angiocoxite; ap = anterior process; b = bursa; c = colpocoxite; ll = lateral lamella; mp = medial part; o = operculum; pl = posterior lobe; s = sternum; sa = synangiocoxal base; sl = sternal lamella; t = telopodite; tf = angiocoxal tuft. Drawings by DA (A–E) and MŠ (F–G). Scale bars = 0.2 mm.

together forming a heartlike structure, divided, but appressed to each other, shieldlike, distomesal and lateral margins folded posteriad; each medial part with subdistal posterior lobe (pl), triangular in posterior view; angiocoxites posteroproximally with a pair of tufts (tf) with hairlike outgrowths and a rounded lobe, covered by spiculiform outgrowths, from which a ridge, also covered with spiculiform outgrowths, continues and fuses with the posterior side of the medial part. Lateral lamellae low, rather wide in lateral view, with slightly denticulate margins. Anterior processes (ap) tapering distad, acuminate, twice as high as lateral lamellae. Coxal vesicles not observed.

Posterior gonopods (Figs 8G, 10D–E). Gonopodal sternum (s) wide, well-developed. Angiocoxites (a) positioned posteriorly, well-developed, slender, curved anterolaterad, longer than colpocoxites (c). Colpocoxites in anterior and posterior views wide in proximal half, then abruptly narrow to half their width in the distal half; fused with basal half of angiocoxites. Telopodites (t) small, rounded, placed posteriorly at base of angiocoxites.

Leg pair 2 in females (Fig. 8A). Coxae with distomesal protrusions covered with small tubercles and setae.

Vulvae (Figs 9G–I, 10F–G). Slightly longer than wide. Operculum (o) well-developed, bilobed, with 5+5 setae (4+4 lateral shorter setae and 1+1 mesal longer setae). Bursa (b) with strongly thickened anteroproximal lips on which the operculum rests. Lateral valve with six setae only in anterior part, mesal valve with 11 or 12 setae.

Locality and ecology

Devis Khvreli is a small horizontal cave 50–60 m long, but as the entrance is relatively small, the whole cave being dark. The cave consists of two parts, a first dry part connected to a second wet part by a narrow passage. This cave is poor in speleothems.

The specimens were found crawling on the substrate or on dead wood in the second, dark and wet part of the cave. Besides the new species, this cave is inhabited by two other millipedes, the troglobiotic *Leucogeorgia gioi* Antić & Reip, 2020 (Antić & Reip 2020) and the troglophilous *Trachysphaera orientalis* Golovatch, 1976 (unpubl. data).

Based on the ecology, the completely unpigmented body and the reduced number of pale brownish ommatidia, *A. devi* sp. nov. can be considered as a neotroglobiont.

Distribution

A Georgian endemic known only from its type locality, Devis Khvreli Cave, near Rgani village (Chiatura Municipality) (Fig. 22, violet circle).

Acanthophorella valerii Antić sp. nov.
urn:lsid:zoobank.org:act:B24D09EE-1BDA-4F40-A853-F3280C49DD7B
Figs 1G–H, 11–16, 21F, 22

Diagnosis

Distinguished from congeners and members of the genus *Pseudoflagellophorella*, except for *A. barjadzei* and *A. devi* sp. nov., by a whitish and unpigmented body (vs pigmented body in others). From both latter it differs by the presence of 10–13 black ommatidia (vs a mainly smaller number of transparent to pale brownish ommatidia in *A. barjadzei* and *A. devi*). Additionally, from *A. barjadzei* and *A. devi*. *Acanthophorella valerii* sp. nov. differs in the general shape of the anterior gonopods, the angiocoxites of the posterior gonopods being short, poorly developed (vs angiocoxites well-developed and strong in *A. barjadzei* and *A. devi*), the coxal processes of leg-pair 7 without lateral lobe (vs lateral lobe present in *A. barjadzei* and *A. devi*) and leg-pair 10 with well-developed coxal processes (vs leg-pair 10 without or with strongly reduced coxal protrusions only in *A. devi*, or with strong protrusions in *A. barjadzei*).

Etymology

The new species is named after Valeri Barbakadze, a Georgian speleologist, cave diver and rescuer. He was an excellent and safe driver, guide and photographer of the cave interior, landscapes and our work during the 2022 expedition to Georgian caves. An interesting thing that gives this name a special charm happened right in front of the type locality of this species, the Usholta Cave. At one point, all members of the expedition came out of the cave, except Valeri, who was still photographing the interior. After a while, the youngest member of the expedition, Luka Barjadze, became worried about Valeri (or most likely about who would drive us back) and started calling him and shouting 'Valeriiiii'. As there is a river running through the cave, Valeri could not hear the call, so the youngster persistently repeated 'Valeriiiii... Valeriiiii'. 'Valeriiiii' could (still) be heard hundreds of metres from the cave entrance. The epithet, a name in the genitive case, is a patronym.

Material examined (2 ♂♂, 1 ♀, 8 juvs)

Holotype

GEORGIA • ♂; Racha, Oni Municipality, Racha karst massif, Usholta village, Usholta Cave; 1772 m a.s.l.; 25 Jul. 2022; D. Antić, E. Kiria, L. Shavadze and S. Barjadze leg.; NHMW MY10366.

Paratypes

GEORGIA • 1 ♂, 1 ♀ (used for SEM); same collection data as for holotype; IZB • 8 juvs; same collection data as for holotype; IZISU.

Description

Size and number of body rings. Body with 31 rings (including telson). Holotype male 15 mm long, vertical diameter of the largest ring 1.10 mm. Paratype male 14 mm long, vertical diameter of the largest ring 1.0 mm. Paratype female 15 mm long, vertical diameter of the largest ring 1.25 mm.

Coloration (Figs 1G–H, 11). Living animals dirty white, with white legs and antennae and black ommatidia.

Head (Figs 11B–D, 12A–D). Setose, roundly convex in females, in males with labral and frontal surfaces flat with convexity between and a pair of poorly developed lateral lobes, each below antennal sockets. Labrum with three medial teeth and 4+4 labral and 2+2 supralabral setae. Promentum triangular, without setae. Lamellae linguales with 8+8 setae. Stipites with ca 30 setae each. Antennae 2.6 mm long in paratype male. Length of antennomeres (in mm): I (0.1), II (0.25), III (0.74), IV (0.34), V (0.7), VI (0.21), VII (0.21) and VIII (0.05). Length/breadth ratios of antennomeres I–VII: I (1), II (1.7), III (6.7), IV (3.1), V (4.6), VI (1.4) and VII (1.8). Antennomeres II, IV, V, VI and VII with one, three, one, four and one long sensillum trichoideum, respectively. Antennomere 7 with one rather bacilliform sensillum (sensillum basiconicum?) curved distad, located below sensillum trichodeum (Fig. 12C). Lateral to antennal sockets, a group of papilliform outgrowths present. Number of ommatidia: 10–13 in 3–4 rows, arranged in elongated triangles (Figs 11B–C, 12B, D).

Collum. Narrower than head, with six macrochaetae as all body rings. Anterior edge semi-circular, posterior margin gently concave.

Body rings (Figs 11A, E–F, 12E–H). With well-developed lateral keels, anterior margins rounded in dorsal view. Macrochaetae long and rather trichoid (Fig. 12F). CIX (ring 15) = 0.6; MIX (ring 15) ~ 1.6; PIX (ring 15) = 0.5; MA (ring 15) ~ 100°.

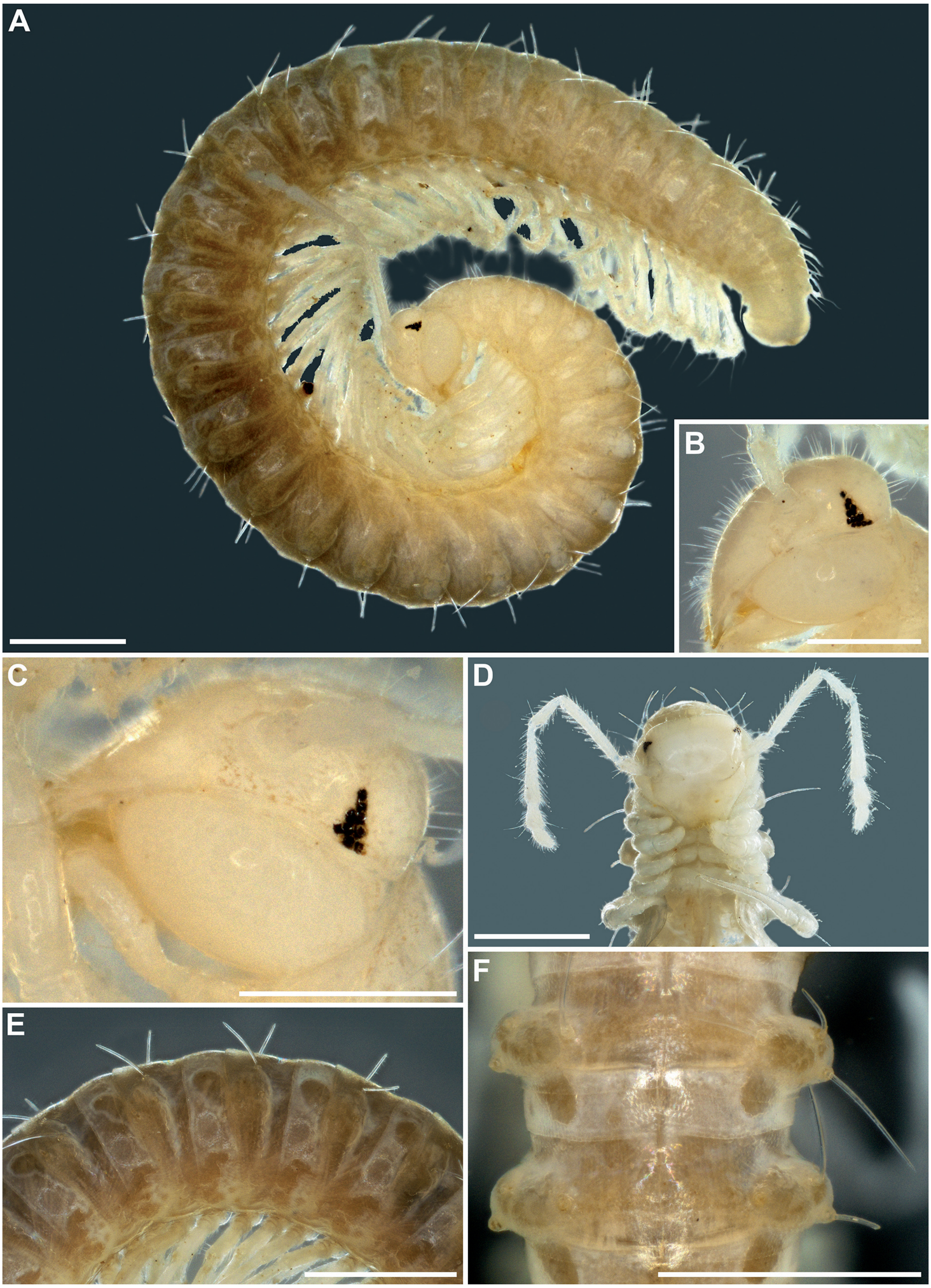

Fig. 11. *Acanthophorella valerii* Antić sp. nov. **A**, **C**, **E**, **F**. Holotype, ♂ (NHMW MY10366). **B**. Paratype, ♀ (IZB). **D**. Paratype, ♂ (IZB). **A**. Habitus, lateral view. **B**. Head, lateral view. **C**. Head, lateral view. **D**. Anterior part of the body, anterior and ventral view. **E**. Midbody rings, lateral view. **F**. Rings 15 and 16, dorsal view. Scale bars: A, D–F = 1 mm; B–C = 0.5 mm.

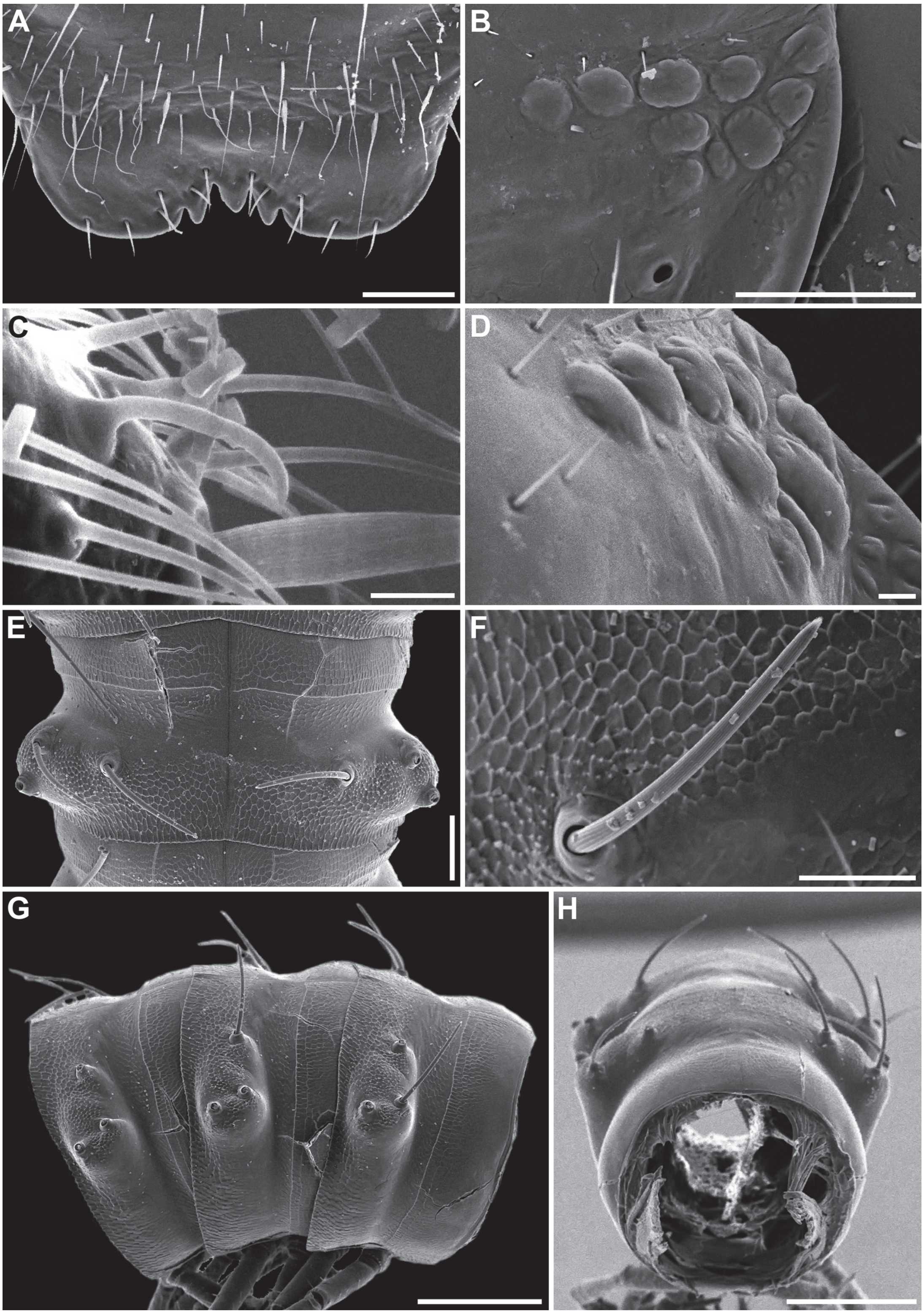

Fig. 12. *Acanthophorella valerii* Antić sp. nov., paratype, ♂ (IZB). **A**. Labrum, anterior view. **B**. Left field with ommatidia and organ of Tömösvary, lateral view. **C**. Left antennomere 7, showing bacilliform sensillum. **D**. Left field with ommatidia, anterior view. **E**. Ring 15, dorsal view. **F**. Right interior macrochaeta of ring 15, dorsal view. **G**. Rings 14–16, dorsolateral view. **H**. Rings 14 and 15, anterior view. Scale bars: A–B, F = 0.1 mm; C–D = 0.01 mm; E = 0.2 mm; G, H = 0.5 mm.

Telson. Epiproct with a pair of spinnerets and 3+3 setae (1+1 paramedian, 2+2 marginal). Hypoproct with 1+1 distal setae. Paraprocts with 3+3 marginal setae in distal part.

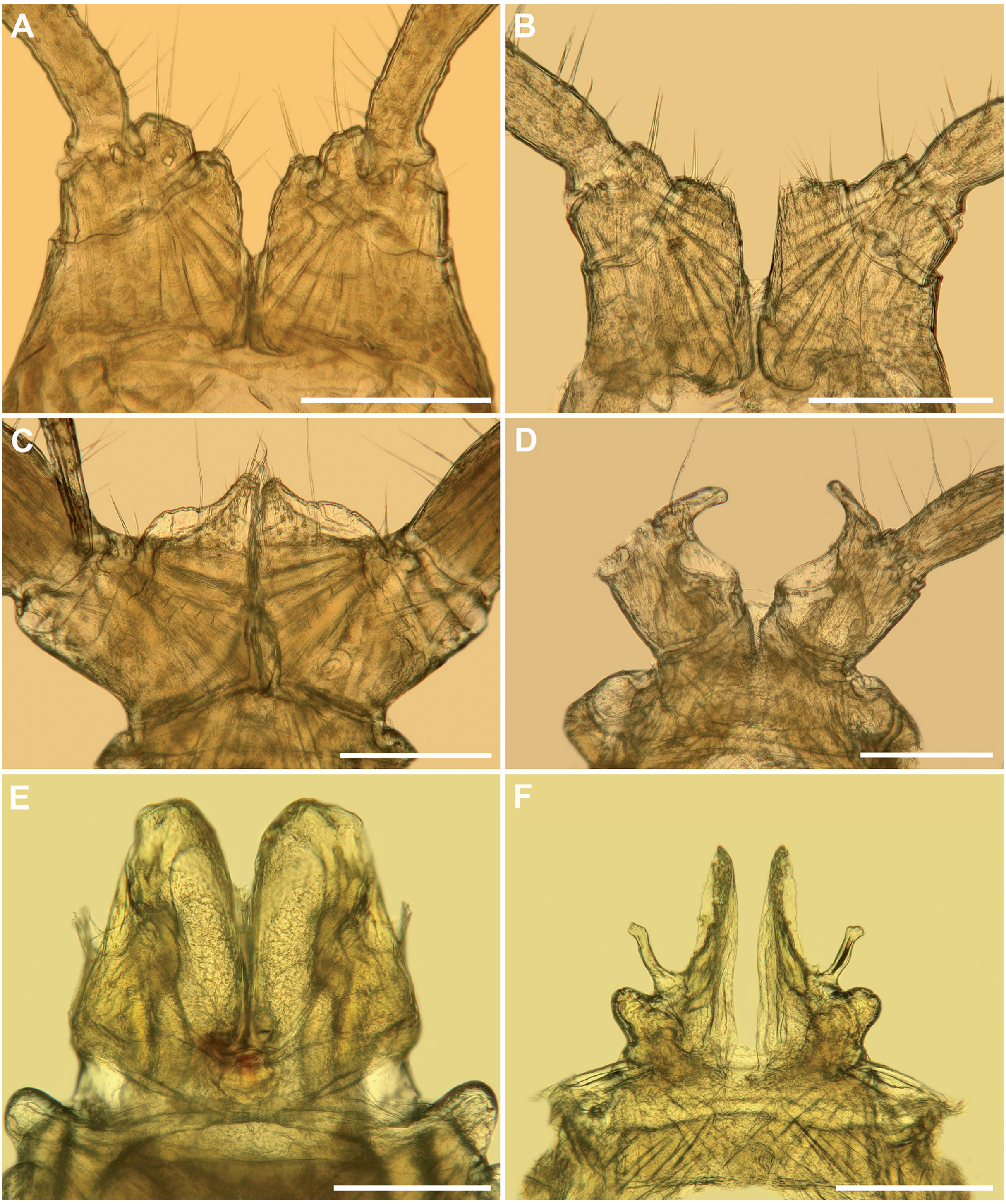

Fig. 13. *Acanthophorella valerii* Antić sp. nov. **A**. Paratype, ♀ (IZB). **B**–**F**. Paratype, ♂ (IZB). **A**. Leg-pair 2, anterior view. **B**. Leg-pair 2, posterior view. **C**. Leg-pair 7, posterior view. **D**. Leg-pair 10, anterior view. **E**. Anterior gonopods, anterior view. **F**. Posterior gonopods, posterior view. Scale bars = 0.2 mm.

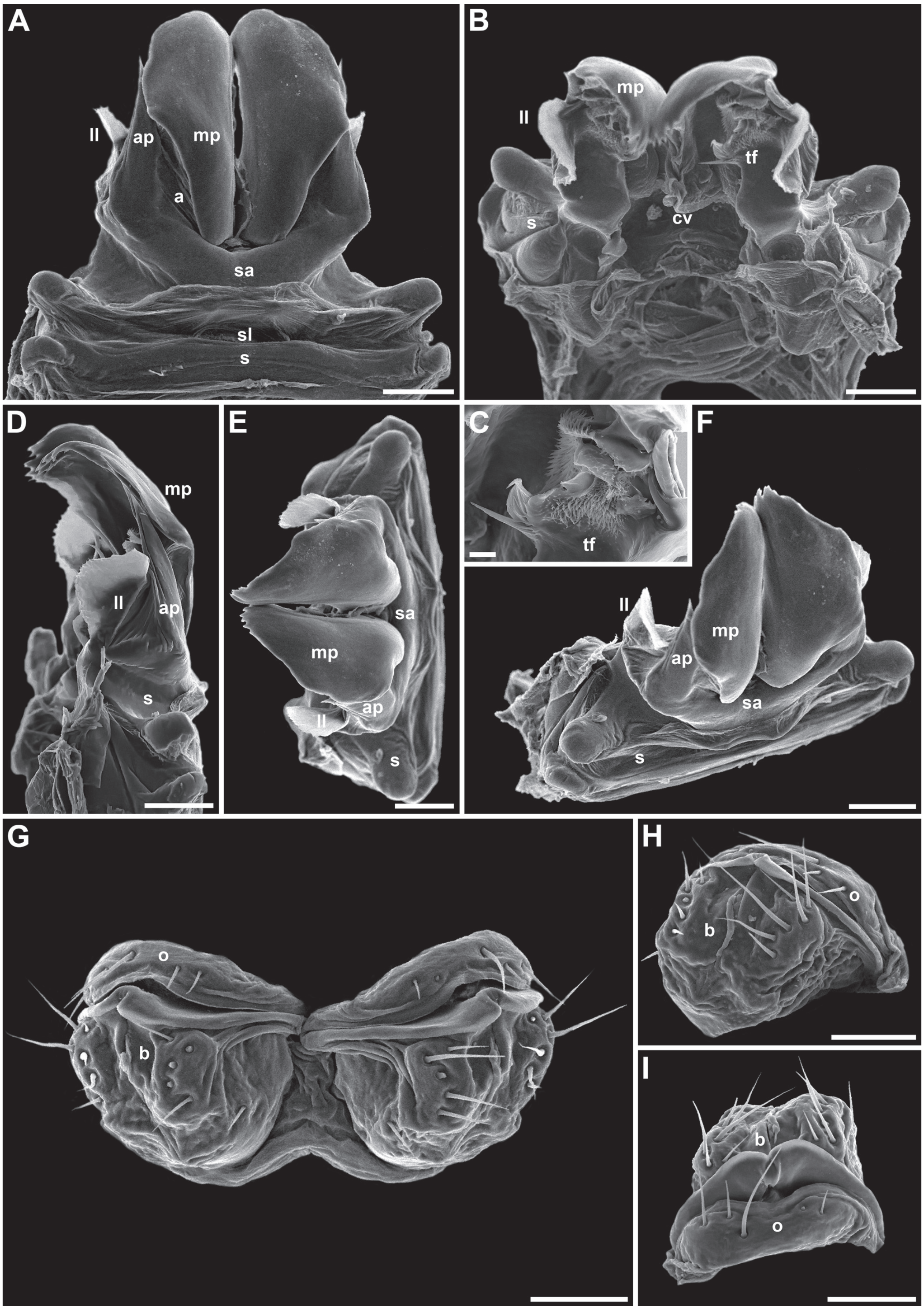

Fig. 14. *Acanthophorella valerii* Antić sp. nov. **A**–**F**. Paratype, ♂ (IZB). **G**–**I**. Paratype, ♀ (IZB). **A**. Anterior gonopods, anterior view. **B**. Anterior gonopods, posterodistal view. **C**. Anterior gonopods, left tuft, posterodistal view. **D**. Anterior gonopods, lateral view. **E**. Anterior gonopods, distal view. **F**. Anterior gonopods, laterodistal view. **G**. Vulvae, distal view. **H**. Left vulvae, lateral view. **I**. Left vulvae, anterior view. Abbreviations: a = angiocoxite; ap = anterior process; b = bursa; cv = syncoxal vesicle; ll = lateral lamella; mp = medial part; o = operculum; s = sternum; sa = synangiocoxal base; sl = sternal lamella; tf = angiocoxal tuft. Scale bars: A–B, D–I = 0.1 mm; C = 0.02 mm.

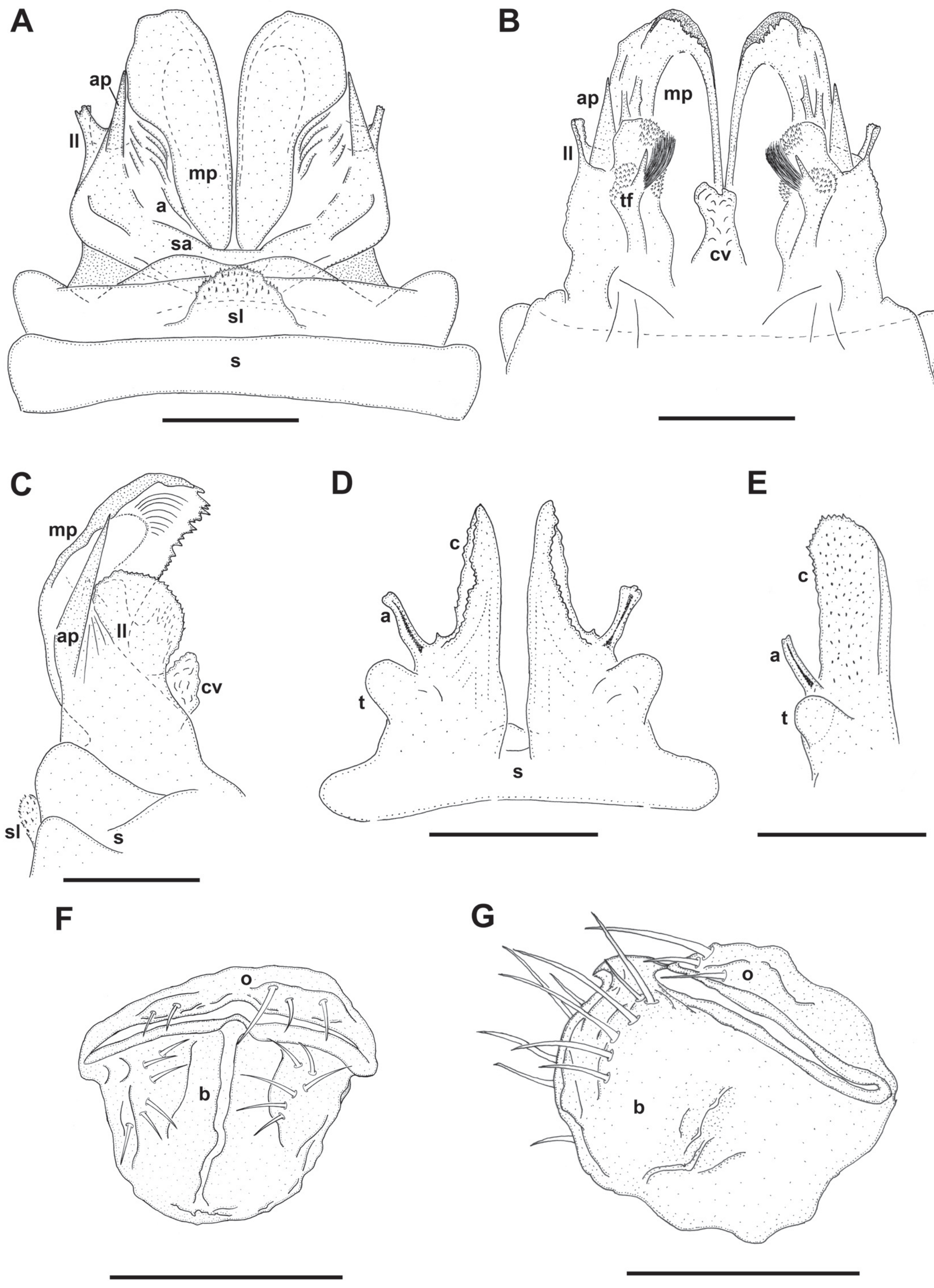

Fig. 15. *Acanthophorella valerii* Antić sp. nov. **A**–**E**. Paratype, ♂ (IZB). **F**–**G**. Paratype ♀ (IZB). **A**. Anterior gonopods, anterior view. **B**. Anterior gonopods, posterior view. **C**. Anterior gonopods, lateral view. **D**. Posterior gonopods, posterior view. **E**. Left posterior gonopod, lateral view. **F**. Left vulva, distal view. **G**. Left vulva, lateral view. Abbreviations: a = angiocoxite; ap = anterior process; b = bursa; c = colpocoxite; cv = syncoxal vesicle; ll = lateral lamella; mp = medial part; o = operculum; s = sternum; sa = synangiocoxal base; sl = sternal lamella; t = telopodite; tf = angiocoxal tuft. Drawings by DA (A–E) and MŠ (F–G). Scale bars = 0.2 mm.

Leg-pairs 1 and 2. In both sexes with tarsal combs; femora, postfemora and tibiae with long and robust setae.

Male sexual characters (Figs 1G–H, 13B–D). Gonopores mesally on coxae 2 (Fig. 13B). Leg-pairs 3–7 enlarged, especially leg-pairs 3, 4 and 7 (Fig. 1G, H). Leg-pairs 3 and 4 very thick, each with a proximal lateral protrusion on prefemora; prefemora and femora strong, rectangular; tarsi shorter and thicker compared to other legs; femora, postfemora and tibiae each with a distoventral pad. Leg-pair 5 with a proximal, anterior, triangular, coxal protrusion. Leg-pair 6 without peculiarities. Leg-pair 7 robust; coxae with wide, well-developed, flattened posterior processes, covered with long setae anteriorly and each with a mesal tooth (Fig. 13C). Leg-pair 10 with coxal glands and well-developed coxal processes oriented posteriad (Fig. 13D). Leg-pair 11 with coxal glands, no other peculiarities.

Anterior gonopods (Figs 13E, 14A–F, 15A–C, 21F). Gonopodal sternum (s) wide, medially with a moderately developed and poorly fimbriate lamella (sl) on anterior side and a bilobed membranous part above. Angiocoxites (a) consisting of a medial part (mp), lateral lamellae (ll) and a synangiocoxal base with anterior processes (ap). Medial parts well-developed, ear-shaped, divided, but appressed to each other, shieldlike, distomesal margins strongly denticulate posteriorly; angiocoxites posteroproximally with a pair of tufts (tf) with longer and shorter hairlike outgrowths, with a spinelike process and a rounded lobe, covered by spiculiform outgrowths. Lateral lamellae low, wide and spoon-shaped in lateral view, with denticulate margins. Anterior processes (ap) tapering distad, acuminate, twice as high as lateral lamellae. A syncoxal vesicle (cv) present posteriorly.

Posterior gonopods (Figs 13F, 15D–E). Gonopodal sternum (s) wide, well-developed. Angiocoxites (a) positioned posteriorly, poorly developed, short, much smaller than colpocoxties (c). Colpocoxites

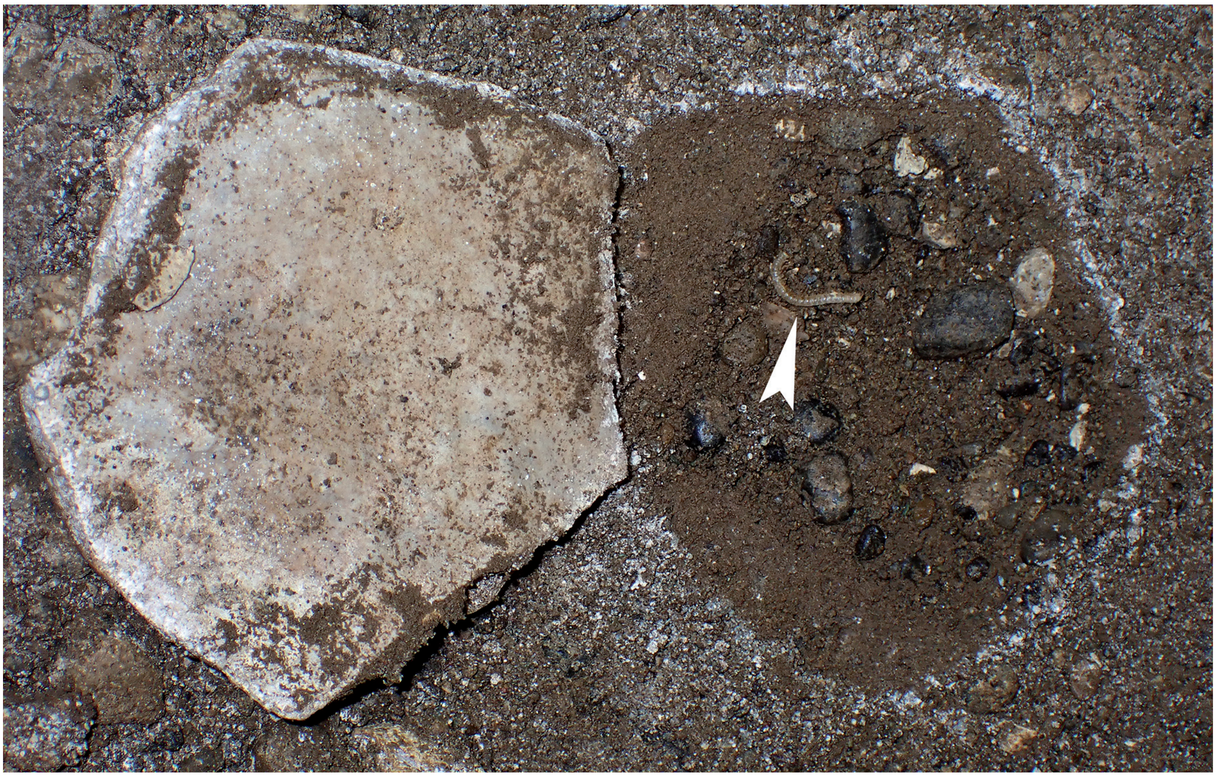

Fig. 16. Dead adult specimen of *Acanthophorella valerii* Antić sp. nov. under the stone on the bank of the cave stream. Photo by Dragan Antić.

strongly developed, tapering in anterior and posterior views, but wide and spoon-shaped in lateral view; margins denticulate. Telopodites (t) small, rounded, placed posterolaterally.

Leg pair 2 in females (Fig. 13A). Coxae with poorly developed distomesal protrusions covered with a few small tubercles and setae.

Vulvae (Figs 14G–I, 15F–G). Rounded, as long as wide. Operculum (o) well-developed, bilobed, lateral lobe with three, mesal with two setae. Bursa (b) with strongly thickened anteroproximal lips on which the operculum rests. Lateral valve with a rounded lobe carrying six setae, mesal valve with a rounded lobe carrying five setae with an additional seta below the lobe.

Locality and ecology

The Usholta Cave, formed in the Lower Cretaceous limestones, is characterised by 2200 m of explored channels, with a permanent water flow in the main channel (Tatashidze *et al.* 2009). This part is poor in speleothems and is mainly characterised by a sandy and gravelly bottom. The deeper, side channels without permanent water flow are rich in speleothems and a clay substrate.

Although many juveniles (only eight were collected) were observed in the dark and damp parts of the cave in all parts explored, exclusively on or in dead wood, only three living adults were found and all three under the stones in the main channel on the banks of the stream. Interestingly, about a dozen dead adults were also found under the stones in the same main channel (Fig. 16). This could mean that at the time of our visit (end of July) the life cycle of the adults was coming to an end and that it is possible that for some reason the adults go under the stones before they die, considering that all of them (both live and dead) were found exclusively under the stones near the stream.

Until now, this cave was very poorly studied in terms of its fauna, as only two common Palaearctic insect species from the families Formicidae Latreille, 1809 and Geometridae Leach, 1815 were recorded (Barjadze *et al.* 2015). Besides *A. valerii* sp. nov., two other troglobionts from the genera *Neobisium* Chamberlin, 1930 (Pseudoscorpiones) and *Inotrechus* Dolzhanski & Ljovuschkin, 1989 (Coleoptera) were found in the cave, as well as the troglophiles *Micropterna clavata* Martynov, 1916 and *Stenophylax permistus* McLachlan, 1895 (both Trichoptera) and a species from the genus *Plutomurus* Yosii, 1956 (Collembola; one juvenile can be spotted in Fig. 1G) (unpubl. data).

Based on the ecology, as well as the unpigmented body, this species can be considered as a neotroglobiont.

Distribution

A Georgian endemic known only from its type locality, Usholta Cave, near Usholta village (Oni Municipality) (Fig. 22, orange circle).

Previously described species and their ecology

Acanthophorella barjadzei Antić & Makarov, 2016
Figs 1A–D, 17–20, 21B, 22

Acanthophorella barjadzei Antić & Makarov, 2016: 143, figs 118–120.

Material examined

Topotypes

GEORGIA • 2 juvs; Racha-Lechkhumi and Kvemo Svaneti Region, Ambrolauri Municipality, Racha karst massif, Velevi village, Dolabistavi Cave; 1170 m a.s.l.; 15 Jun. 2019; H. Reip, J. Hentschel, L. Binz and E. Göbel leg.; SMNG • 2 juvs; same cave as for preceding; 25 May 2022; S. Barjadze, A. Faille and E. Maghradze; SMNS.

Additional material

GEORGIA – **Racha-Lechkhumi and Kvemo Svaneti Region** • 1 ♂, 1 ♀, 1 juv.; Ambrolauri Municipality, Racha karst massif, Nikortsminda village, Nikortsminda Sakinule Cave; 1196 m a.s.l.; 24 Jul. 2022; D. Antić, E. Kiria, L. Shavadze and S. Barjadze leg.; IZB • 1 ♂, 1 ♀; same collection data as for preceding; NHMW MY10367 • 1 ♂; same collection data as for preceding; IZISU • 2 ♂♂, 6 ♀♀ (one used for SEM), 1 juv.; same cave as for preceding; 14 Jun. 2019; H. Reip, J. Hentschel, L. Binz and E. Göbel leg.; SMNG • 2 ♂♂ (one used for SEM), 1 ♀, 3 juvs; Muradi Cave; 1500 m a.s.l.; 24 Jul. 2022; D. Antić, E. Kiria, L. Shavadze and S. Barjadze leg.; IZB • 2 ♀♀, 2 juvs; same cave as for preceding; 18 Oct. 2021; J. Grego and R. Straub leg.; IZISU.

Remarks

As more males and females are now available for *A. barjadzei*, we provide some additional descriptive notes here (Figs 17–20). Males 19–23.5 mm long, vertical diameter of the largest ring 1.40–1.50 mm. Females 17.5–26 mm long, vertical diameter of the largest ring 1.40–1.70. Head and gnathochilarium densely setose (Figs 17B, 18A). Antennomere 7 with one rather bacilliform sensillum (sensillum basiconicum?) curved distad, located below sensillum trichodeum (Fig. 18D). Lateral to antennal sockets, a group of papilliform outgrowths present. Number of ommatidia 5–10, but mainly 5–7, in 2–3 rows, arranged in elongated triangles; ommatidia pale brownish or completely transparent (Figs 1A, C, 17A–B, D, 18B). In one female, the number of ommatidia is 9+10. Leg-pairs 3 and 4 in males with femoral, postfemoral and tibial distoventral pads. Leg-pair 10 in males with a rounded or subtriangular, distal, coxal protrusion, but also with a triangular, posterior, proximal, coxal protrusion. The anterior and posterior gonopods of the males from Muradi and Nikortsminda Sakinule caves almost completely agree with the gonopods of the holotype from Dolabistavi Cave. Angioxocal tufts (tf) (= hairy levers + lobes) complicated, including lobes with long and short hairlike outgrowths and spiculiform outgrowths, distally with an opening (Fig. 19E–F). The only difference spotted between males from Muradi and Nikortsminda Sakinule caves compared to the holotype is the presence of much shorter lateral lamellae (Fig. 19A, F) in males from the two mentioned caves. Leg-pair 2 in females with well-developed distomesal protrusions on coxae covered with small tubercles and setae. Vulvae (Figs 19G–I, 20) with anterior part as wide as vulval length. Operculum (o) well-developed, bilobed, with 6+6 setae (5+5 lateral shorter setae and 1+1 mesal longer setae). Bursa (b) with strongly thickened anteroproximal lips on which the operculum rests. Lateral valve with eight setae, mesal valvee with nine setae. Posteriorly, bursa with wrinkled lateral lobe.

Localities and ecology

The type locality, Dolabistavi Cave, like other caves in the Racha karst massif, is formed in Cretaceous limestone. The explored length of the cave is 140 m, with a depth of 20 m (Tatashidze *et al.* 2009). The cave is characterised by narrow passages without speleothems, and with a stream in the lower level, which is the source of the Khoteura River. Until this study, *A. barjadzei* was only known from its type locality. Antić & Makarov (2016) stated that this species probably lives also in Muradi Cave, but in the absence of adult males they left the identification to future studies. Now that we have adult males at hand, we can confirm *A. barjadzei* from Muradi and Nikortsminda Sakinule caves. Muradi Cave is another high altitude cave with a low and wide entrance (4 × 1 m). The cave has 660 m of investigated channels and is characterised by two levels, a lower and an upper, separated by a 10 m vertical passage. From the entrance, the cave descends steeply to the lower level. The temperature in the cave is 7°C. This is one of the most famous caves in Georgia in terms of speleothems, which are very numerous and diverse in the upper level (Asanidze *et al.* 2017). The most interesting and unique among them are certainly the pool speleothems (https://www.youtube.com/watch?v=z2TfqQEUxMA). Nikortsminda Sakinule is a 100 m long and 15 m deep cave that is poor in speleothems but well known for its ice formations and low temperature (Tatashidze *et al.* 2009). From the huge entrance the cave slopes steeply downwards. This part of the cave is mainly characterised by lined boulders and stones. From the lower part of the cave, a steep ascent leads to the second part, which is much wetter and with a mostly clay substrate.

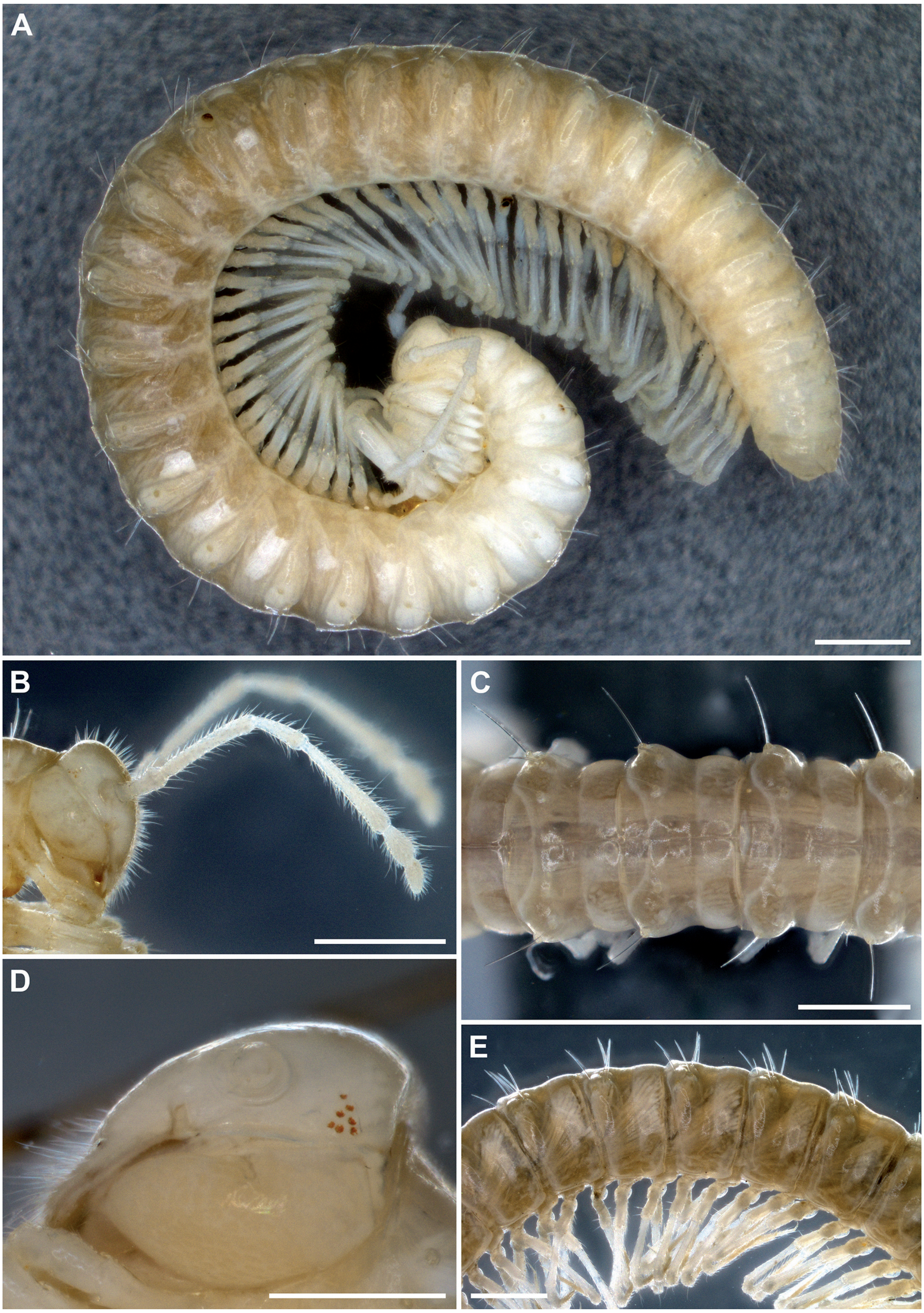

Fig. 17. *Acanthophorella barjadzei* Antić & Makarov, 2016. **A**. ♂ from Nikortsminda Sakinule Cave, habitus, lateral view (NHMW MY10367). **B**. ♀ from Nikortsminda Sakinule Cave, head, lateral view (NHMW MY10367). **C**. ♂ from Muradi Cave, midbody rings, dorsal view (IZB). **D**. Subadult ♀ from Muradi Cave, head, lateral view (IZISU). **E**. ♂ from Muradi Cave, midbody rings, lateral view (IZB). Scale bars: A–C, E = 1 mm; D = 0.5 mm.

In Dolabistavi Cave, specimens of *A. barjadzei* were found in the dark parts, crawling around on the wet rocks. In Muradi Cave, specimens were found in the lower part of the cave (we did not explore the upper part), walking and probably feeding on wet dead wood. In Nikortsminda Sakinule Cave, specimens were found between near the entrance and the second, completely dark part of the cave. All animals were

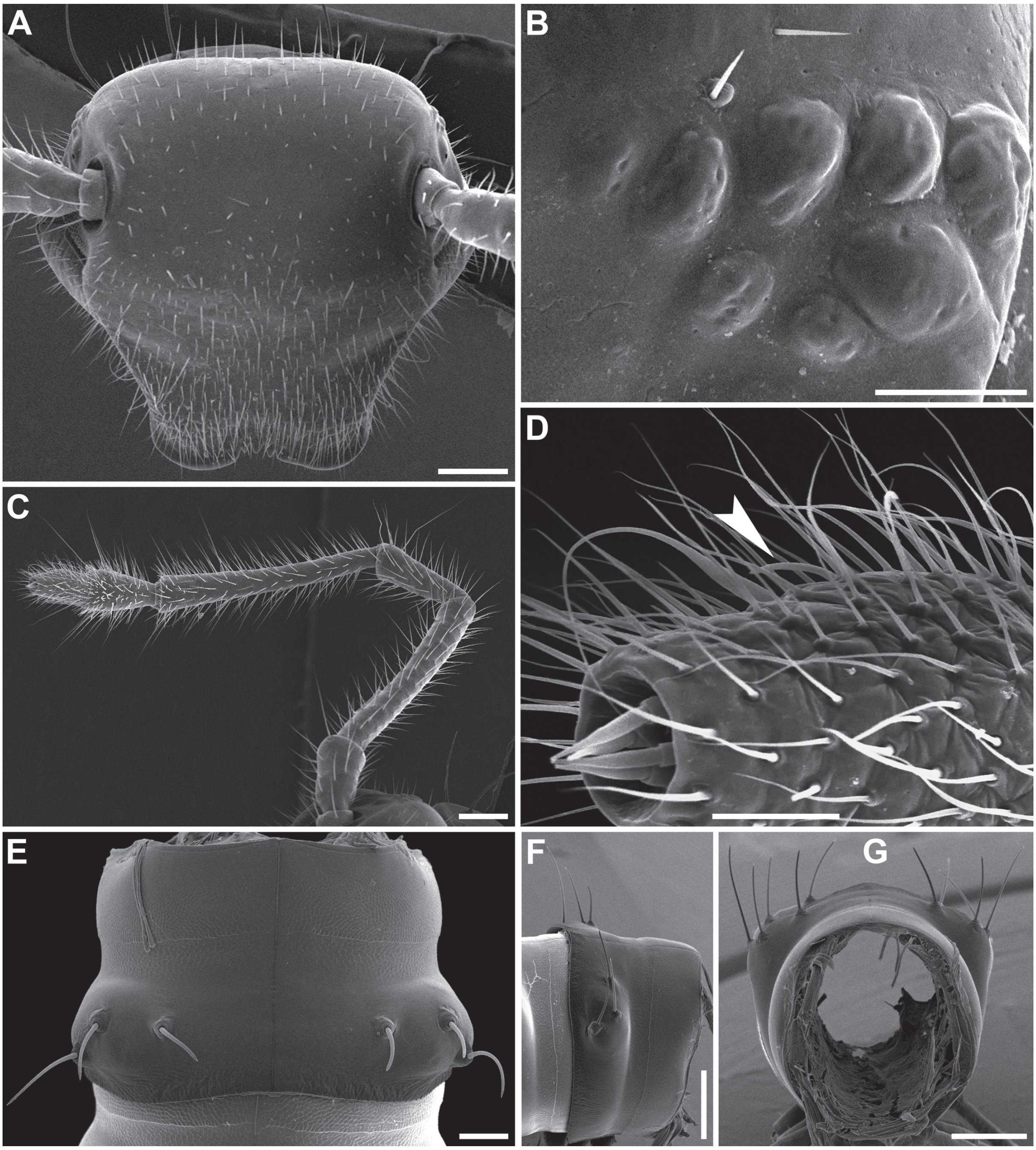

Fig. 18. *Acanthophorella barjadzei* Antić & Makarov, 2016, ♂ from Muradi Cave (IZB). **A**. Head, anterior view. **B**. Left field with ommatidia, anterolateral view. **C**. Right antenna, dorsal view. **D**. Right antennomere 7, dorsal view, arrow indicates bacilliform sensillum. **E**. Ring 14, dorsal view. **F**. Ring 14, dorsolateral view. **G**. Rings 14 and 15, anterior view. Scale bars: A, C, E = 0.2 mm; B, D = 0.05 mm; F–G = 0.5 mm.

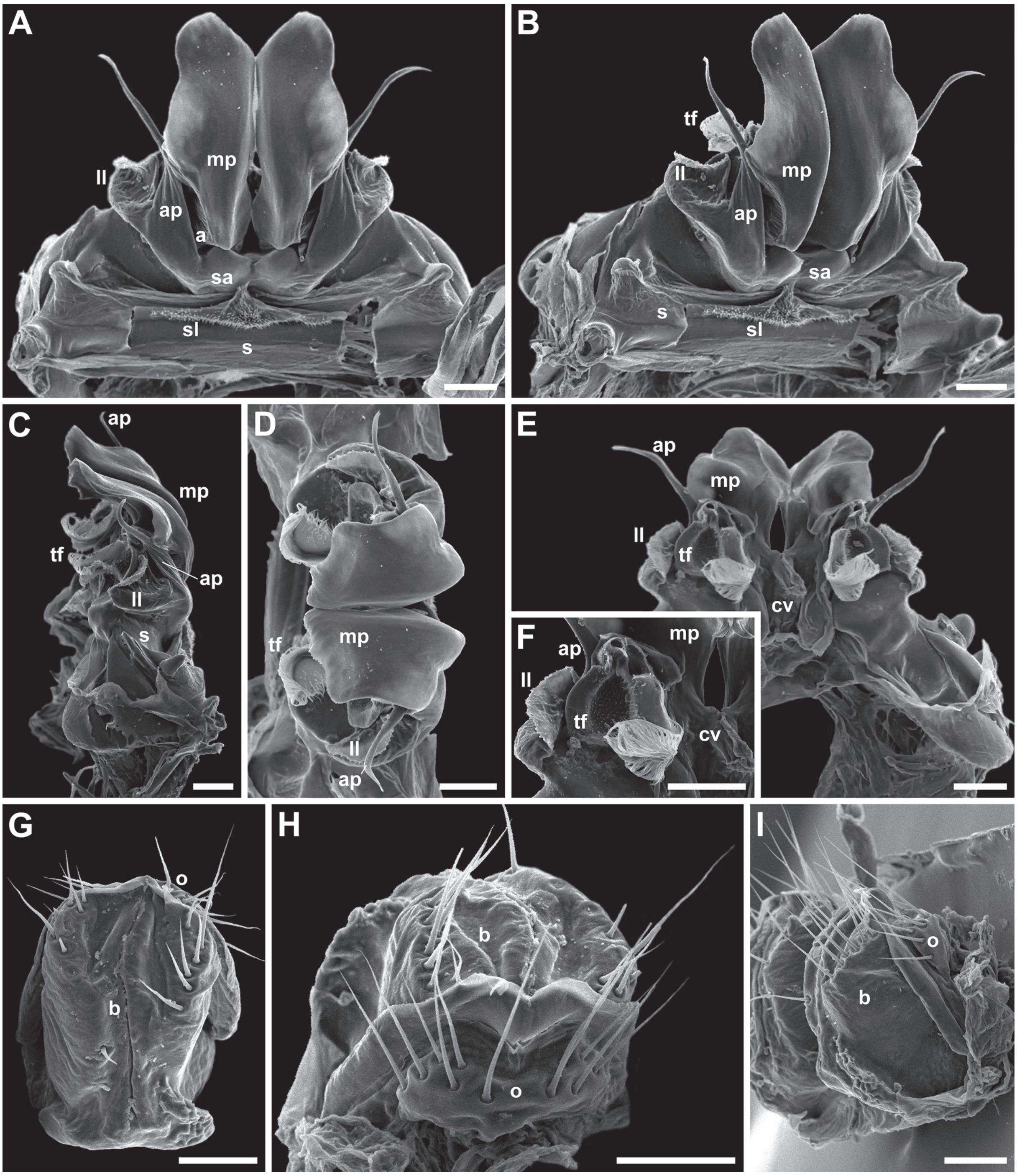

Fig. 19. *Acanthophorella barjadzei* Antić & Makarov, 2016. **A–F**. ♂ from Muradi Cave (IZB). **G–I**. ♀ from Nikortsminda Sakinule Cave (SMNG). **A**. Anterior gonopods, anterodistal view. **B**. Anterior gonopods, anterolaterodistal view. **C**. Anterior gonopods, lateral view. **D**. Anterior gonopods, distal view. **E**. Anterior gonopods, posterior view. **F**. Anterior gonopods, right tuft, posterior view. **G**. Left vulva, distal view. **H**. Left vulva, anterodistal view. **I**. Left vulva, lateral view. Abbreviations: a = angiocoxite; ap = anterior process; b = bursa; cv = coxal vesicle; ll = lateral lamella; mp = medial part; o = operculum; s = sternum; sa = synangiocoxal base; sl = sternal lamella; tf = angiocoxal tuft. Scale bars = 0.1 mm.

found in the left part of the cave, which is almost in complete darkness and characterised by very wet and cold stones. The specimens mainly walked on the stones covered with green algae or on dead wood or deeper on clay. Some were feeding on algae, as the green colour was clearly visible in the gut.

Besides *A. barjadzei*, another troglobiotic millipede inhabiting all three caves is the hydrophilous *Leucogeorgia longipes* Verhoeff, 1930 (Antić & Reip 2020 for Dolabistavi; unpublished for Muradi and Nikortsminda Sakinule). One more interesting, stygobiotic species from Dolabistavi Cave is the recently described, *Hausdorfenia pseudohauffenia* Grego & Mumladze, 2020 (Gastropoda) (Grego *et al.* 2020). For additional taxa known from Dolabistavi Cave see Barjadze *et al.* (2015). In Nikortsminda Sakinule Cave, five mite and one springtail species have been recorded so far (Barjadze *et al.* 2015). During the expedition, we registered additional four troglobionts from the genera *Neobisium* (Pseudoscorpiones), *Nemaspela* Šilhavý, 1966 (Opiliones), *Inotrechus* (Coleoptera) and *Pseudosinella* Schäffer, 1897 (Collembola) (unpubl.). In Muradi Cave, besides two troglobiotic millipede species, we registered two troglophiles, viz., *Micropterna clavata* and *Stenophylax permistus* (both Trichoptera) (unpubl.).

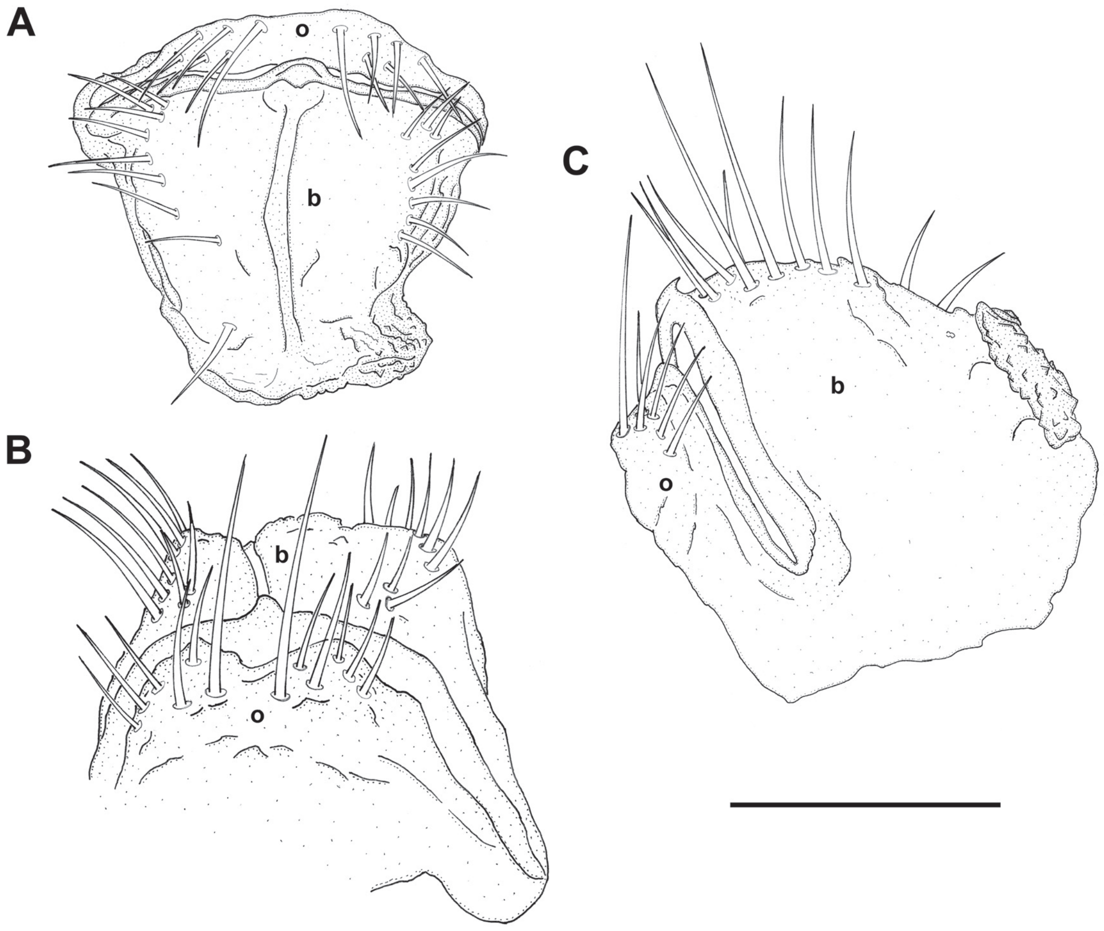

Fig. 20. *Acanthophorella barjadzei* Antić & Makarov, 2016, ♀ from Nikortsminda Sakinule Cave (**S**MNG). **A**. Left vulva, distal view. **B**. Left vulva, anterior view. **C**. Right vulva, lateral view. Drawings by MŠ. Abbreviations: b = bursa; o = operculum. Scale bar = 0.2 mm.

Based on the ecology, the unpigmented body and the unpigmented or pale brownish and reduced number of ommatidia, *A. barjadzei* can be considered as a troglobiont. Furthermore, this species is characterised by a more robust and larger body (cave gigantism), compared to its congeners. With a length of up to 26 mm, *A. barjadzei*, together with the members of the troglobiotic genus *Heterocaucaseuma* Antić & Makarov, 2016, is the largest chordeumatidan in the Caucasus.

Distribution

A Georgian endemic known from three high-altitude caves (ca 1200–1500 m a.s.l.) in the Racha karst massif (Fig. 22, cyan circles).

Acanthophorella chegemi Antić & Makarov, 2016
Fig. 21C, 22

Acanthophorella chegemi Antić & Makarov, 2016: 147, figs 121–125.

Remarks and distribution

Epigean species. Russian endemic so far known only from the type series collected at Upper Chegem, Kabardino-Balkaria. The specimens were collected in the litter and under stones at 1700 m a.s.l. in *Betula*-, *Pinus*- and *Juniperus*-vegetation or at timber-line of *Betula-, Rhododendron-* and *Juniperus*-vegetation, 2100–2200 m a.s.l. (Antić & Makarov 2016) (Fig. 22, red circle).

Acanthophorella irystoni Antić & Makarov, 2016
Fig. 21E, 22

Acanthophorella irystoni Antić & Makarov, 2016: 152, figs 126–128.

Acanthophorella irystoni – Golovatch & Antipova 2022: 134, 140.

Remarks and distribution

Epigean species. Russian endemic so far known only from one locality between Chmi and Baltik in North Ossetia. The specimens were collected in the litter and under stones on a slope with *Quercus* L. and *Alnus* Mill. (Antić & Makarov 2016) (Fig. 22, yellow circle). Considered as being endemic to the Republic of North Ossetia–Alania, north-central Caucasus Major (Golovatch & Antipova 2022).

Key to the species of the Flagellophorella complex

Modified and refined after Antić & Makarov (2016).

1. 29 body rings (including telson) in adults. Angiocoxites of anterior gonopods with a pair of flagella .... ***Flagellophorella hoffmani*** Antić & Makarov, 2016
– 31 body rings (including telson) in adults. Angiocoxites of anterior gonopods with a pair of pseudoflagella, spinelike, tapering, mostly acuminate processes or hidden processes 2

2. Angiocoxites with a pair of hidden processes, with only distal parts visible ....***Crypthacanthophorella manubriata*** Antić & Makarov, 2016
– Angiocoxites with visible pseudoflagella or spinelike acuminate processes, only partly covered with mesal parts of the angiocoxites 3

3. Angiocoxites with very long and slender pseudoflagella of equal thickness over the entire extent, forming a semi-circular curvature first and then rising distad .... ***Pseudoflagellophorella*** Antić & Makarov, 2016 (4)
– Angiocoxites with rather stubby, tapering and mostly acuminate spinelike processes arising from synangiocoxal base directly distad without making a proximal curvature .... ***Acanthophorella*** Antić & Makarov, 2016 (6)

4. Proximal parts of angiocoxites very wide and rounded .... ***P. eskovi*** Antić & Makarov, 2016
– Proximal parts of angiocoxites not rounded, same width as the rest 5

5. Angiocoxites with fimbriate lateral parts showing numerous single, bi- or triramous fringes/fingers orientated posteriad. Sternal lamella well-developed, fimbriate .... ***P. mirabilis*** Antić & Makarov, 2016
– Anterior gonopods with neither fimbriated lateral parts nor fringes/fingers. Sternal lamella poorly developed with only distal margin fimbriated ....***P. papilioformis*** Antić & Makarov, 2016

6. Unpigmented, whitish species. Presumed troglobionts 7
– Pigmented, epigean species 9

7. Ommatidia black .... ***A. valerii*** Antić sp. nov.
– Ommatidia pale brownish or transparent, sometimes barely visible 8

8. Large species, 16–26 mm long (usually about 20 mm). Macrochaetae long and trichoid. Coxal processes of leg-pair 7 in males with a mesal tooth. Coxae of leg-pair 10 with strong subtriangular or rounded protrusions. ....***A. barjadzei*** Antić & Makarov, 2016
– Smaller species, 11–13 mm long. Macrochaetae shorter and bacilliform. Coxal processes of leg-pair 7 in males without mesal tooth. Coxae of leg-pair 10 without or with only a poorly visible protrusion .... ***A. devi*** Antić sp. nov.

9. Angiocoxites of posterior gonopods wide, ear-shaped ....***A. aurita*** Antić sp. nov.
– Angiocoxites of posterior gonopods neither wide nor ear-shaped 10

10. Lateral lamellae of angiocoxites of anterior gonopods as high as medial parts of angiocoxites. Angiocoxites of posterior gonopods well developed, hook-shaped, curved anteriad ....***A. chegemi*** Antić & Makarov, 2016
– Lateral lamellae of anterior gonopods distinctly lower than medial parts. Coxal processes of posterior gonopods small, columnar .... ***A. irystoni*** Antić & Makarov, 2016

To easily distinguish all nine species of the genera *Acanthophorella* and *Pseudoflagellophorella*, see also Figure 21.

Discussion

Notes on the relationships within the *Flagellophorella* complex

The genus *Acanthophorella* is presently the most species-rich genus within the *Flagellophorella* complex, with six species involved. The genus *Pseudoflagellophorella* includes three species, while *Flagellophorella* and *Cryptacanthophorella* are monospecific. As mentioned above, with the discovery and description of three new species of *Acanthophorella*, the differences between the genera of the *Flagellophorella* complex become less clear. This is especially true for the genera *Acanthophorella* and *Pseudoflagellophorella*. In the past, apart from the structure of the anterior processes (explained above in the diagnosis of and remarks to *Acanthophorella*), there were some other features that distinguished these two genera such as the presence of a small and poorly developed sternal lamella of the anterior gonopods in *Acanthophorella*, vs a well-developed sternal lamella in *Pseudoflagellophorella*, or the presence of only coxal protrusions or very small coxal processes on male leg-pair 10 in *Acanthophorella*, vs long, well-developed coxal processes of leg-pair 10 in *Pseudoflagellophorella*. Now these characters can no longer be used to distinguish those genera. On the one side, *A. aurita* sp. nov. is characterised by anterior processes and lateral lamellae of the anterior gonopods as in the genus *Acanthophorella*, but on the other hand, the presence of a well-developed sternal lamella is characteristic of the genus *Pseudoflagellophorella*. Similarly, *A. valerii* sp. nov. also has anterior processes and lateral lamellae of the *Acanthophorella* type, the sternal lamella is transitional between the genera *Acanthophorella* and *Pseudoflagellophorella*, while the coxae of leg-pair 10 are characterised by the presence of well-

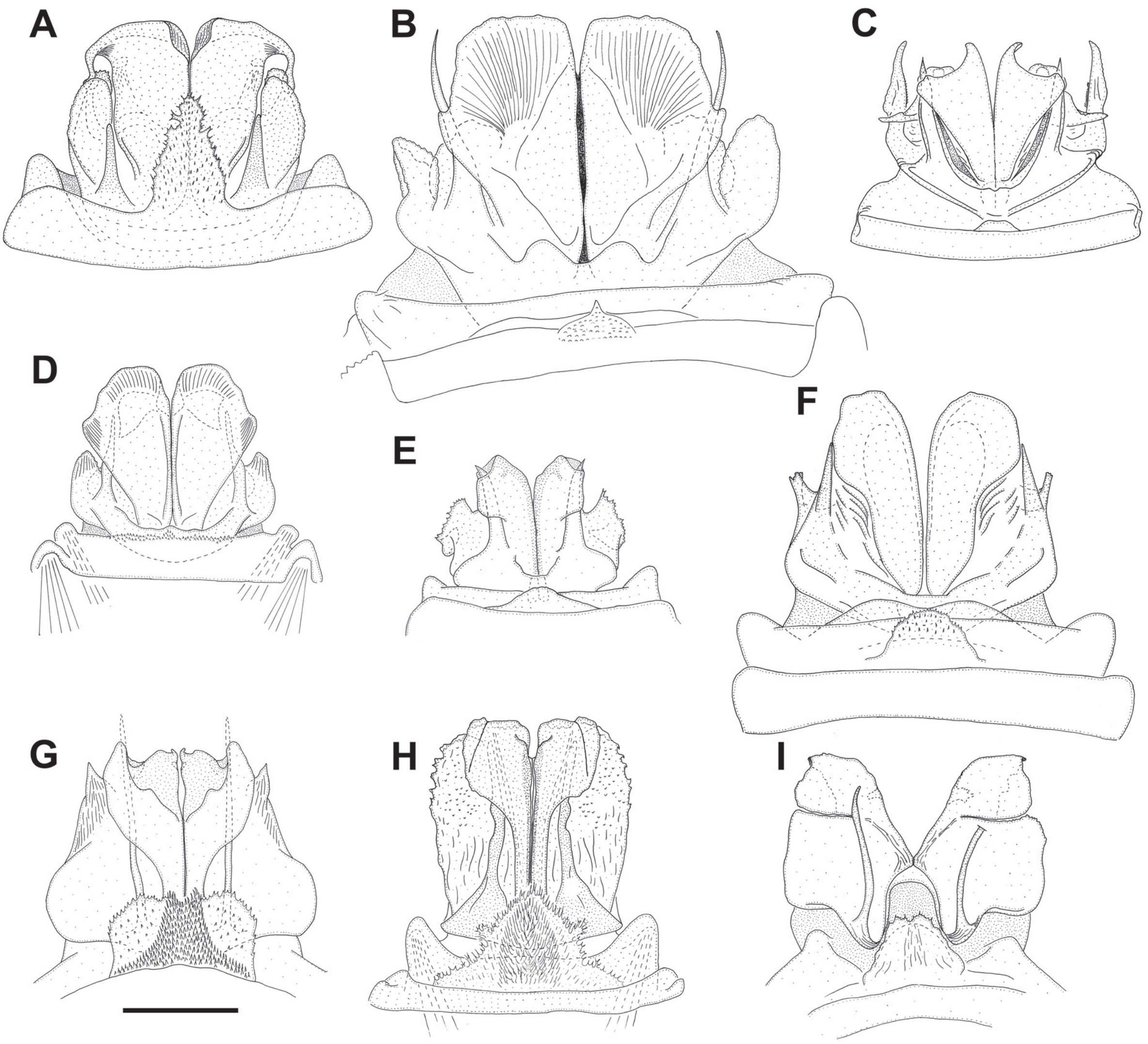

Fig. 21. Anterior gonopods in the genera *Acanthophorella* Antić & Makarov, 2016 and *Pseudoflagellophorella* Antić & Makarov, 2016, anterior views. **A**. *A. aurita* Antić sp. nov. **B**. *A. barjadzei* Antić & Makarov, 2016. **C**. *A. chegemi* Antić & Makarov, 2016. **D**. *A. devi* Antić sp. nov. **E**. *A. irystoni* Antić & Makarov, 2016. **F**. *A. valerii* Antić sp. nov. **G**. *P. eskovi* Antić & Makarov, 2016. **H**. *P. mirabilis* Antić & Makarov, 2016. **I**. *P. papilioformis* Antić & Makarov, 2016. B–C, E, G–I after Antić & Makarov (2016). Scale bar = 0.2 mm.

developed processes as in the genus *Pseudoflagellophorella*. Finally, it should be mentioned that the coxal protrusions/processes of leg-pair 10 in *A. devi* sp. nov. are either completely absent or barely discernible. In this sense, all character states in the coxae of leg-pair 10 can now be detected in the genus *Acanthophorella*, from well-developed processes, through well or less developed protrusions, to the complete absence of any structure. It is clear from the above that some species of the genus *Acanthophorella* share the characteristics of the genera *Acanthophorella* and *Pseudoflagellophorella*. Therefore, the boundary between these two genera is now very shaky and it is very likely that it will disappear with new discoveries and descriptions in the future.

The validity of the genus *Cryptacanthophorella* is also questionable. Some characters of the anterior gonopods, such as the general shape of the medial parts, the structure of the lateral lamellae and the poorly developed sternal lamella, show similarities with most species of the genus *Acanthophorella*. However, the anterior processes, which we have used here as the only character to distinguish the genera, are almost completely hidden in the angiocoxites, with only the distal third protruding and visible in lateral view only. We are not excluding the possibility that all three previously mentioned genera will prove to be synonyms in the future.

The fourth genus of the *Flagellophorella* complex is the monospecific genus *Flagellophorella*. It appears that this genus is well established, as it is clearly distinguished from the other three genera by the presence of a pair of flagella on the anterior gonopods with free proximal halves, while the distal halves lie within the longitudinal ribs of the angiocoxites and by the presence of a strongly developed, high sternal lamella on the anterior gonopods protecting the proximal parts of the flagella. In addition, it is characterized by the presence of 29 body rings in adults (including telson) vs 31 in the other three genera.

It is worth mentioning that there is another member of the very heterogeneous family Anthroleucosomatidae, *Anamastigona matsakisi* Mauriès & Karamouna, 1984 from the island of Naxos in Greece, which is characterised by a pair of anterior flagella or pseudoflagella on the anterior gonopods (Mauriès & Karamouna 1984). Although the anterior and posterior gonopods are relatively similar to some members of the *Flagellophorella* complex, it is not possible to say whether they are phylogenetically close or merely convergently similar taxa. Perhaps at some point in the future it will be possible to test this, but it will always be a challenge to re-collect taxa described in the past.

Notes on the distribution of the genus *Acanthophorella*

Members of the genus *Acanthophorella* are confined exclusively to the Caucasus Major, mainly in its central part, on both its northern and southern macro slopes (Fig. 22). Two species, both epigean, viz., *A. chegemi* and *A. irystoni*, are known from a single locality each on the northern slopes of the Russian republics of Kabardino-Balkaria and North Ossetia-Alania, respectively.

The remaining four species inhabit the southern slopes of the Caucasus Major in western Georgia. The epigean *A. aurita* sp. nov. has possibly the largest distribution in the genus, with the type locality in the Colchis lowlands near the Black Sea coast and a potential locality in the Racha karst massif. It is interesting to note that each of the three troglobiont representatives of this genus is restricted to a small area in the easternmost part of the limestone strip of western Georgia. *Acantophorella barjadzei* is known from three high altitude caves above Lake Shaori in the central and southern parts of the Racha karst massif. *Acantophorella valerii* sp. nov. is also a high-altitude cave inhabitant of the Racha karst massif, but is confined to its easternmost part. Finally, *A. devi* sp. nov. is present in the Zemo Imereti Plateau. Another new (based on gonopod photos), presumably troglobiotic species of the genus *Acanthophorella* was found on the same plateau in Kotia Cave, located ca 10 km southeast of the site of *A. devi*. Unfortunately, this sample containing male(s) is considered lost in the IZISU collection. During our expedition we found many juveniles and one female of this new species, but not a single male. Interestingly, in addition to the troglobiotic species of *Acanthophorella*, there is another presumed troglobiont, *Ratcheuma excorne* Golovatch, 1985, in the karst massif of Racha. It seems that in the northwest this core of cave-dwelling *Acanthophorella* from the Racha karst massif and the Zemo Imereti Plateau is replaced by the troglobiotic *Georgiosoma* Antić & Makarov, 2016, from the *Caucaseuma* complex. This monospecific genus is known from the neighbouring Khvamli karst massif, which is separated from the Racha karst massif by the Rioni River. It is worth mentioning that juveniles and/or females of apparently cave-dwelling chordeumatidans have also been found in the caves of the Sataphlia-Tskaltubo karst massif, which is located west of the Racha massif and the Zemo Imretei Plateau. It will be interesting to see in the future whether these animals are related to the genus *Acanthophorella*/*Flagellophorella* complex or to something else.

Notes on troglomorphism in the genus *Acanthophorella*

Together with *Caucaseuma* with eight species, *Acanthophorella*, now with six species, is the most diverse chordeumatidan genus in the Caucasus. At the same time, these are the only two genera of Caucasian chordeumatidans that contain both epigean and troglobiotic forms. As already noted by Antić & Makarov (2022), there are still no cave chordeumatidans in the Caucasus characterised by the complete absence of ommatidia. Moreover, some presumed troglobiotic taxa are endowed with a large number of ommatidia, as can be seen in the genera *Caucaseuma* and *Heterocaucaseuma* Antić & Makarov, 2016 (Antić & Makarov 2016, 2022; Antić *et al.* 2018). The presence of ommatidia also characterises all three presumed troglobiotic *Acanthophorella* species. It is worth mentioning that their adaptation process to the cave environment may still be underway. As far as troglomorphic features within the genus are concerned, *A. valerii* sp. nov. seems to show the least degree of adaptation to cave habitats. This species is characterised by a dirty white body, with completely white legs and antennae, but a rather large number (10–13) of completely black ommatidia. The next level of adaptation could be seen in *A.*

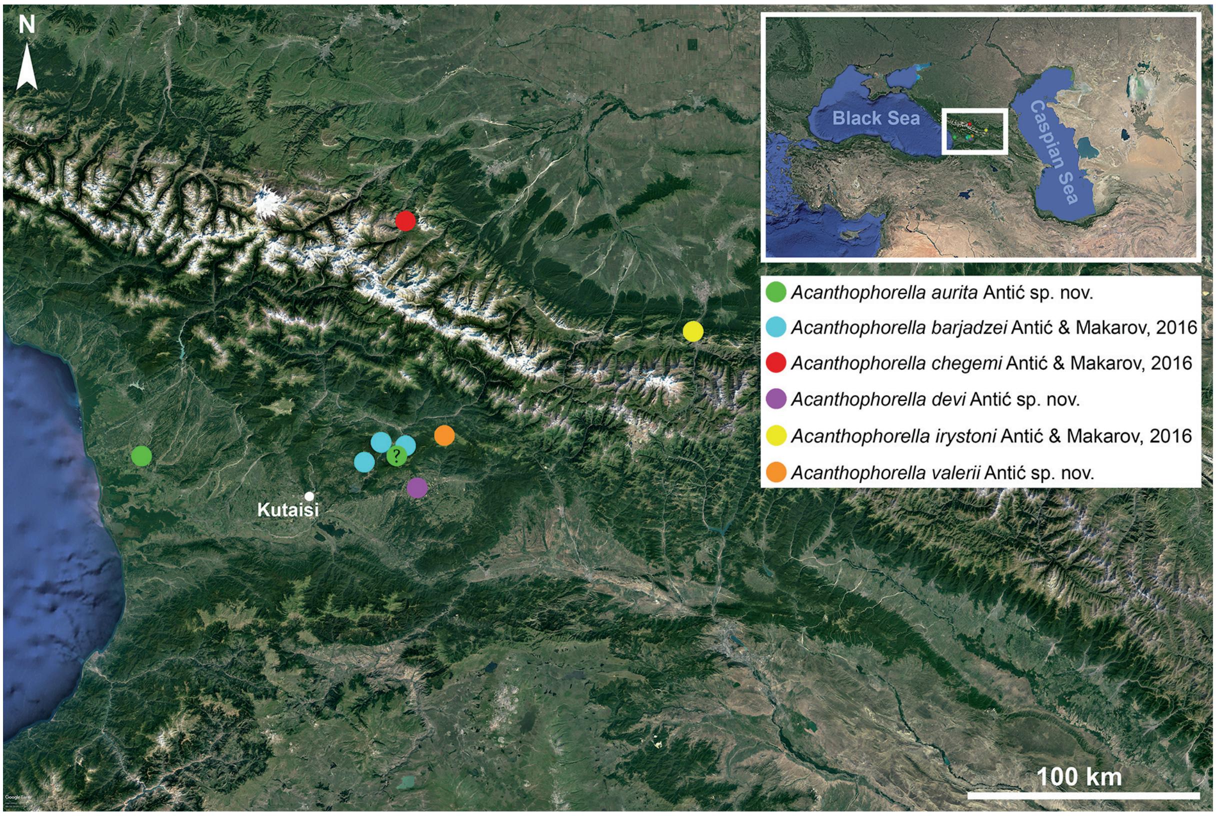

Fig. 22. Distribution of the genus *Acanthophorella* Antić & Makarov, 2016.

devi sp. nov. which is characterised by a completely unpigmented, white body and a smaller number (5–7) of light brown ommatidia. Based on the presence of some troglomorphies as well as ecology, both previously mentioned species can be considered as neotroglobionts. Finally, *A. barjadzei* seems to have gone the furthest. This species is very robust and one of the largest chordeumatidans in the Caucasus, which could be an example of cave gigantism. In addition, this taxon is characterised not only by the somewhat elongated legs, unpigmented white body, densely setose head and gnathochilarium, but also by a reduced number and pigmentation of ommatidia. The number of ommatidia in this species ranges from 5 to 10, but in most cases it is 5–7. It is interesting that both individuals with light brown ommatidia and individuals with completely transparent ommatidia can be found within the same population. At the moment it seems that *A. barjadzei* is one of the Caucasian chordeumatidan species with the highest degree of morphological adaptations to cave conditions.

With the two newly described neotroglobionts, the number of cave-dwelling anthroleucosomatids in the Caucasus has increased to 14. The family Anthroleucosomatidae and the tribe Leucogeorgiini Verhoeff, 1930, which includes 15 presumed troglobionts (Antić & Reip 2020; Antić & Turbanov 2022), are by far the richest millipede groups in terms of the number of troglobionts in Caucasian caves. As intensive and extensive biospeleological research is underway across the territory of Georgia, the number of Caucasian troglobionts is expected to increase in the near future.

Acknowledgements

We are very grateful to all collectors mentioned in the Material examined sections for the specimens provided. DA and SB are immensely grateful to Valeri Barbakadze, Eleonora Kiria, Lado Shavadze and Luka Barjadze (all Georgia) for their company, help and fun during the excursion to the Georgian caves. For the foregoing, SB is also indebted to Arnaud Faille (Germany) and Eter Maghradze (Georgia). We also thank Marko Radenković and Miloš Bokorov (University Centre for Electron Microscopy, Department of Biology and Ecology, University of Novi Sad, Serbia) for the help with SEM photographs and Katarina Stojanović (IZB) for identifying the Trichoptera specimens. We owe a great deal of gratitude to the reviewers Sergei Golovatch (Russia), William Shear (USA) and Henrik Enghoff (Denmark) as well as to the editor Nesrine Akkari (Austria) for their helpful suggestions and corrections. Last but not least, DA is exceptionally thankful to all the Georgians he met along the way for their great hospitality, which made him feel at home.

The field trip of DA and SB to Georgian caves in 2022 was funded by the National Geography Society grant under the project "Revealing the subterranean biodiversity of Georgia (Caucasus Mts)" (Grant No. NGS-93344R-22) and by the Van Tienhoven Foundation under the project: "Investigation and conservation of the cave dwelling invertebrates, their habitats and education of local communities on the cave conservation in Racha karst massif, Georgia, Caucasus" (Grant No. 22109). The work was partially supported by the Serbian Ministry of Science, Technological Development and Innovation (Grant No. 451-03-47/2023-01/ 200178).

References

Antić D.Ž. & Makarov S.E. 2016. The Caucasus as a major hotspot of biodiversity: evidence from the millipede family Anthroleucosomatidae (Diplopoda, Chordeumatida). *Zootaxa* 4211 (1): 1–205. https://doi.org/10.11646/zootaxa.4211.1.1

Antić D.Ž. & Makarov S.E. 2022. Review of the genus *Caucaseuma* Strasser, 1970, with the description of a new cavernicolous species from the Western Caucasus and an updated key and distribution (Diplopoda, Chordeumatida, Anthroleucosomatidae). *European Journal of Taxonomy* 819: 90–107. https://doi.org/10.5852/ejt.2022.819.1783

Antić D.Ž. & Reip H.S. 2020. The millipede genus *Leucogeorgia* Verhoeff, 1930 in the Caucasus, with descriptions of eleven new species, erection of a new monotypic genus and notes on the tribe Leucogeorgiini (Diplopoda: Julida: Julidae). *European Journal of Taxonomy* 713: 1–106. https://doi.org/10.5852/ejt.2020.713

Antić D. & Turbanov I.S. 2022. An unexpected new cave-dwelling species of the genus *Leucogeorgia* Verhoeff, 1930 (Diplopoda: Julida: Julidae) from the Chechen Republic, Caucasus, Russia. *Arthropoda Selecta* 31 (4): 375–383. https://doi.org/10.15298/arthsel.31.4.01

Antić D.Ž., Turbanov I.S. & Reboleira A.S.P.S. 2018. From the depths: *Heterocaucaseuma deprofundum* sp. nov., the world's deepest-occurring millipede (Diplopoda, Chordeumatida, Anthroleucosomatidae) from caves in the western Caucasus. *Zootaxa* 4377 (1): 110–124. https://doi.org/10.11646/zootaxa.4377.1.7

Asanidze L., Lezhava Z. & Chikhradze N. 2017. Speleological Investigation of the Largest Limestone Massif in Georgia (Caucasus). *Open Journal of Geology* 7: 1530–1537. https://doi.org/10.4236/ojg.2017.710102

Barjadze S., Murvanidze M., Arabuli T., Mumladze L., Pkhakadze V., Djanashvili R. & Salakaia M. 2015. *Annotated List of Invertebrates of the Georgian Karst Caves*. Georgian Academic Book, Tbilisi.

Golovatch S.I. & Antipova M.D. 2022. The millipedes (Diplopoda) of the Republic of North Ossetia – Alania, northern Caucasus, Russia, with special reference to the fauna of the North Ossetian Nature Reserve. *Arthropoda Selecta* 31 (2): 133–142. https://doi.org/10.15298/arthsel.31.2.01

Grego J., Mumladze L., Falniowski A., Osikowski A., Rysiewska A., Palatov D.M. & Hofman S. 2020. Revealing the stygobiotic and crenobiotic molluscan biodiversity hotspot in Caucasus: Part I. The phylogeny of stygobiotic *Sadlerianinae* Szarowska, 2006 (Mollusca, Gastropoda, Hydrobiidae) from Georgia with descriptions of five new genera and twenty-one new species. *ZooKeys* 955: 1–77. https://doi.org/10.3897/zookeys.955.51983

Mauriès J.-P. & Karamaouna M. 1984. Myriapodes-Diplopodes nouveaux et peu connus des îles Naxos, Paros et Antiparos (Cyclades, Grèce). *Biologia gallo-hellenica* 11: 51–59.

Tatashidze Z.K., Tsikarishvili K.D. & Jishkariani J.M. 2009. *The Cadastre of the Karst Caves of Georgia*. Petiti Publishing House, Tbilisi. [In Georgian.]

Manuscript received: 10 March 2023
Manuscript accepted: 9 June 2023
Published on: 17 November 2023
Topic editor: Magalie Castelin
Section editor: Nesrine Akkari
Desk editor: Pepe Fernández

Printed versions of all papers are also deposited in the libraries of the institutes that are members of the *EJT* consortium: Muséum national d'histoire naturelle, Paris, France; Meise Botanic Garden, Belgium; Royal Museum for Central Africa, Tervuren, Belgium; Royal Belgian Institute of Natural Sciences, Brussels, Belgium; Natural History Museum of Denmark, Copenhagen, Denmark; Naturalis Biodiversity Center, Leiden, the Netherlands; Museo Nacional de Ciencias Naturales-CSIC, Madrid, Spain; Leibniz Institute for the Analysis of Biodiversity Change, Bonn – Hamburg, Germany; National Museum of the Czech Republic, Prague, Czech Republic.